New Phytologist

Research

Exogenous sugar addition can exacerbate root carbon limitation in trees

Yan-Li Zhang[1,2], Arthur Gessler[1,2], Marco M. Lehmann[1], Marcus Schaub[1], Matthias Saurer[1], Andreas Rigling[1,2] and Mai-He Li[1]

[1]Forest Dynamics, Swiss Federal Institute for Forest, Snow and Landscape Research WSL, CH-8903, Birmensdorf, Switzerland; [2]Department of Environmental Systems Science, Institute of Terrestrial Ecosystems, ETH Zürich, CH-8092, Zürich, Switzerland

Authors for correspondence:
Yan-Li Zhang
Email: yanli.zhang@wsl.ch

Mai-He Li
Email: maihe.li@wsl.ch

Received: *5 March 2025*
Accepted: *22 April 2025*

New Phytologist (2025) **247:** 577–594
doi: 10.1111/nph.70231

Key words: carbon allocation, carbon balance, carbon isotopes, carbon starvation, defoliation, exogenous sugar, leaf gas exchange, leaf senescence.

Summary

- In most tree species, roots serve as major carbon (C) sinks, where C is depleted first when C assimilation is limited. Recent methodological advancements in sugar infusion allow for a better understanding of physiological processes alleviating root C limitation.
- We conducted a glasshouse experiment with maple (*Acer pseudoplatanus* L.) and pine (*Pinus sylvestris* L.) saplings that underwent defoliation followed by either slow, fast, or no ^{13}C-labeled glucose infusion. We measured photosynthetic parameters, nonstructural carbohydrate (NSC) concentrations, and δ^{13}C in cellulose of leaves, twigs, and fine roots, as well as the isotopic composition of dark-respired CO_2.
- Sugar infusion induced photosynthetic downregulation and leaf senescence in maple but not in pine. Leaf photosynthesis was negatively correlated with leaf NSC concentration in maple. These responses exacerbated root C limitation in maple. Conversely, pine maintained stable photosynthetic rates and needle NSC concentrations across treatments, showing the potential of sugar infusion to mitigate root C limitation.
- Our study suggests that exogenous sugar supply reduces the root C availability when it impairs a plant's photosynthetic performance. Species-specific differences influence infused sugar transport and overall source–sink responses. Alleviating C limitation in roots via exogenous sugar addition is feasible only if photosynthesis is not impeded.

Introduction

Climate change increasingly disrupts forest ecosystems' functioning, posing significant threats to tree survival and resilience world-wide (Allen *et al.*, 2010; Hartmann *et al.*, 2018; Brodribb *et al.*, 2020; Groover *et al.*, 2025). One of the most critical impacts of climate change is the rising frequency of defoliation events, driven by factors such as insect outbreaks, drought, and extreme weather events (Anderegg *et al.*, 2015; Senf *et al.*, 2018). By reducing their photosynthetic capacity, defoliation disrupts the carbon (C) balance of trees, depletes nonstructural carbohydrate (NSC) reserves (McDowell *et al.*, 2008), and intensifies C limitation (Barker Plotkin *et al.*, 2021; Z. Wang *et al.*, 2021). This intensified C limitation can impair tree growth, reduce resilience to subsequent stressors, and ultimately increase tree mortality risk (Senf *et al.*, 2021; McDowell *et al.*, 2022; International Tree Mortality Network, 2025).

C limitation under stress often begins in roots, as defoliation and reduced C availability significantly impact C allocation to sink tissues (Landhäusser & Lieffers, 2012). High defoliation can strongly reduce root starch concentrations in Scots pine (*Pinus sylvestris* L.) (Schönbeck *et al.*, 2018), while reduced atmospheric CO_2 causes Norway spruce (*Picea abies* L.) to retain assimilates aboveground at the expense of root supply (Huang *et al.*, 2019). Similarly, drought limits C allocation to roots in Scots pine (Joseph *et al.*, 2020), with a meta-analysis showing that drought decreases root NSC concentrations by 17.3% while leaving aboveground reserves unchanged (W. Li *et al.*, 2018). Comparable patterns have been observed in trees at the cold alpine treeline (M.-H. Li *et al.*, 2018) and in high-elevation shrubs (X. Wang *et al.*, 2021), where colder winter temperatures exacerbate root NSC depletion due to reduced C uptake and metabolic activity. Metabolic analyses indicate that many stress-related metabolites decrease in fine roots but increase in needles of Scots pine when needle loss exceeds 80–85% (Hunziker *et al.*, 2024). Over time, insufficient C investment belowground can shrink the rhizosphere zone, impairing nitrogen and water uptake (e.g. in Scots pine, Gao *et al.*, 2021). Therefore, root C reserves play an important role in tree survival under stresses that cause C limitation (Ouyang *et al.*, 2021; Yang *et al.*, 2022).

Sugar infusion into the stem xylem might be a promising method to mitigate C limitation by supplementing trees with exogenous sugars, which are taken up, translocated, and metabolized (Zhang *et al.*, 2023). Similar approaches have shown potential for alleviating stress-related impacts in various plant species. For instance, sucrose infusion reversed shade-induced kernel

reductions in crops (Hiyane *et al.*, 2010) and mitigated reproductive failure in maize (*Zea mays*) under low water potential conditions during flowering (Boyle *et al.*, 1991). In woody plants, sucrose supplementation through vase solutions delayed tissue deterioration over several days by counteracting carbohydrate depletion in *Protea eximia* (Bieleski *et al.*, 1992). Likewise, trunk carbohydrate injections during dormancy enhanced growth and vitality in oaks (Martínez-Trinidad *et al.*, 2009). Exogenous sucrose injections have also increased sugar and starch levels in citrus leaves and fruits (Iglesias *et al.*, 2002, 2003).

The effectiveness of sugar infusion may depend on the sugar transport, which is influenced by species-specific differences in wood anatomy. These differences stem from variations in parenchyma structure between gymnosperms and angiosperms. Gymnosperms, such as conifers, typically have 5–10% parenchyma in their wood, predominantly composed of ray parenchyma with minimal or no axial parenchyma (Plavcová & Jansen, 2015). By contrast, angiosperms possess 20–40% parenchyma, including both ray and axial parenchyma, which enhances their capacity for efficient storage and transport of substances (Plavcová & Jansen, 2015). This structural difference may influence the amount of sugar utilization and allocation. Additionally, leaf longevity and resource allocation strategies further differentiate these groups (Adler *et al.*, 2014; Reich, 2014; Salguero-Gómez, 2017; Zhang *et al.*, 2020). Conifers, with their long-lived needles that persist through winter, are adapted to store and gradually utilize sugars over an extended period, promoting a more stable C balance, most likely reducing the immediate need for rapid sugar metabolism. By contrast, broadleaved angiosperms have short-lived leaves with higher metabolic activities that senesce within the same growing season. This shorter lifespan and more acquisitive resource use may lead to a more rapid buildup of exogenously supplied sugars.

Despite its potential to alleviate C limitation, sugar infusion might also trigger photosynthetic downregulation due to negative feedback mechanisms. The assimilate inhibition hypothesis posits a negative feedback relationship between leaf NSC concentrations and photosynthetic activity (Neales & Incoll, 1968). This hypothesis is supported by recent studies reporting negative correlations between leaf NSC concentrations and photosynthetic capacity (Ozawa *et al.*, 2023; Tian *et al.*, 2024). The feedback mechanism is thought to involve multiple pathways. As NSCs accumulate in leaves, they signal a reduced demand for photosynthates, prompting the plant to decrease its photosynthetic capacity. This occurs through the suppression of photosynthetic gene expression, reduced activity of key enzymes such as ribulose-1,5-bisphosphate carboxylase/oxygenase (RuBisCO) (Krapp *et al.*, 1991; Moore *et al.*, 1999), and limitations in transporting photosynthates from source to sink tissues (Lemoine *et al.*, 2013). Source tissues, such as mature leaves, generate and export photosynthates, whereas sink tissues, including roots and developing leaves, depend on imported sugars for growth and maintenance. When carbohydrate accumulation disrupts this source–sink balance, photosynthetic gene expression declines, and leaf senescence may be accelerated (Paul & Foyer, 2001). Exogenous sucrose application has been shown to inhibit photosynthesis in sugarcane by downregulating RuBisCO abundance and activity (Lobo *et al.*, 2015). This regulatory mechanism helps plants balance C fixation with whole-plant C demand, optimizing resource allocation and energy efficiency (Körner, 2015). Thus, we might assume that exogenous C supply might not necessarily relieve trees from C depletion but, on the contrary, by reducing photosynthesis and inducing leaf senescence, aggravate it.

This study aimed to investigate how two species with contrasting life strategies respond to sugar infusion under defoliated (C-limited) and nondefoliated (non-C-limited) conditions, with the goal of identifying strategies to alleviate C limitation in trees. We conducted a glasshouse experiment to examine the effects of slow and fast sugar infusion on photosynthesis, NSC concentrations, and structural growth in deciduous broadleaved Sycamore maple (*Acer pseudoplatanus* L.) and evergreen conifer Scots pine. To simulate stress-induced C limitation, we defoliated trees to reduce their photosynthetic capacity and increase C demand. We then infused ^{13}C-labeled glucose solution into the stem xylem at both slow and fast rates (i.e. 'slow sugar infusion' and 'fast sugar infusion') and compared the results to trees infused with distilled water (i.e. 'water infusion'). Following the infusion, we measured photosynthetic parameters, the C isotopic composition of dark-respired CO_2 ($\delta^{13}C_R$), NSC concentrations, and structural growth in the leaves/needles, twigs, and fine roots.

Considering the wood anatomical and functional differences in parenchyma structure between conifers and angiosperms, maple is expected to transport added sugars to its leaves more rapidly and efficiently than pine. This difference is likely due to the higher proportion of axial parenchyma in angiosperms, which facilitates efficient sugar transport, whereas conifers primarily rely on ray parenchyma with limited axial parenchyma (Plavcová & Jansen, 2015). Based on these structural differences, we hypothesized that (i) in maple, sugar infusion leads to leaf NSC accumulation, downregulation of photosynthesis, and induction of senescence. As a result, adding exogenous sugars to the xylem is not relieving but intensifying root C limitation due to the impairment of photosynthesis.

By contrast, the structure of needle leaves may play a role in limiting sugar accumulation in the mesophyll. The mesophyll is separated from the central xylem by an endodermis in the needle leaf. Apoplastic transport of water and solutes (including the transported exogenous sugars) is inhibited (Mai *et al.*, 2024). As a result, sugar accumulation is most likely localized within the central cylinder and does not reach the mesophyll cells where photosynthesis occurs. Consequently, we hypothesized that (ii) pine trees exhibit no significant sugar accumulation in their needles, maintain stable photosynthetic activity, and show potential for mitigating C limitation in their fine roots.

Materials and Methods

Experimental design

Plant materials Three-year-old sycamore maple (*A. pseudoplatanus* L., 170–200 cm in height, 1.0–1.5 cm in diameter at breast height) and 6-yr-old Scots pine (*P. sylvestris* L., 150–180 cm in

height, 1.0–1.5 cm in diameter at breast height) trees were purchased from a local nursery. On 3–4 April 2023, 58 trees for each species were planted in pots (height 30 cm and diameter 35 cm, *c.* 30 l) in the glasshouse at the Swiss Federal Research Institute WSL. At planting, pots were filled with soil provided by the company Ökohum (Herbertingen, Germany; medium and basic mineral fertilization). The trees were exposed to natural daylight throughout the experiment. The photoperiod during the experiment was 14.7 h d^{-1}, and the average light intensity in the glasshouse was 21.2 klx. The average temperature of 22.3°C represents the 24-h mean in the glasshouse, with day and night temperatures averaging 23.9°C and 20.4°C, respectively. The humidity levels averaged 57% throughout the experiment, which lasted until 18 July 2023. Detailed information about glasshouse light, temperature, and humidity can be found in Supporting Information Figs S1, S2. The plants were watered daily to maintain consistent soil moisture, ensuring nonlimiting water conditions.

Treatments ***Defoliation.*** On 10 May 2023, after 36 d of recovery from transplantation, 29 trees of each species were randomly selected for the defoliation treatment (hereafter referred to as C-limited trees), and the other 29 trees remained intact as nondefoliated controls (non-C-limited). All fully expanded leaves were removed from the twigs for C-limited maple trees, and the growing leaves that were not fully expanded were left intact. For C-limited pine trees, all previous years' needles were removed by clipping along the twigs of each branch, and the current year's new needles were left intact.

Infusion. To reduce costs associated with the high price of ^{13}C-labeled glucose and to avoid potential ^{13}C-enrichments in samples above a threshold that could cause problems during analysis, such as memory effects, the sugar solution used for infusion was prepared as a mixture of nonlabeled and ^{13}C-labeled glucose. Before infusion, a nonlabeled glucose solution was prepared by dissolving 1.5 kg of nonlabeled D-glucose powder (Carl-Roth, Karlsruhe, Germany) in 2.25 l of distilled water (*c.* 1 : 1.5 for sugar : water). The resulting concentration of the nonlabeled glucose solution was 3.7 mol l^{-1} (66.7% w/v). We used a relatively high sugar concentration compared to the typical sugar concentration of 1% in the xylem sap (Raven, 1983), assuming the xylem water would continuously dilute the infused sugar. Second, a labeled glucose solution was prepared by dissolving 12.3 g of ^{13}C-labeled D-glucose powder ($^{13}C_6$, 99 atom% ^{13}C, Sigma-Aldrich, Buchs, Switzerland) in 48 ml distilled water (*c.* 1 : 4 for sugar : water). This concentration (1.4 mol l^{-1} or 25.6% w/v) was lower than that of the nonlabeled solution due to the high costs of labeled glucose. Still, the concentration allowed accurate isotopic measurements. The infusion set consisted of a 20-ml syringe and a 120 cm-long rubber tube with a flow regulator (Jiangxi Hongda Medical Apparatus and Instruments Group Company Ltd, Nanchang, China).

Ten days after defoliation treatment, we began infusing the stem xylem with either glucose solution or distilled water. A hole (2.5 mm in diameter and *c.* 0.8 cm deep) was drilled at a 45° angle into the stem xylem (Zhang *et al.*, 2023). Immediately after drilling, the hole was flushed and filled with distilled water using a syringe. We first poured 15 ml of nonlabeled glucose solution into the rubber tube to remove air bubbles. The rubber tube (2.5 mm in diameter) was carefully inserted into the hole, and the joint was sealed with silicone. After 1 h, when the silicone was dry, the infusion tube regulator was turned on. The glucose solution treatment was applied first with 1 ml ^{13}C-labeled glucose solution, followed by 30 ml nonlabeled glucose solution (Fig. 1). The distilled water treatment was carried out with 31 ml of distilled water. These treatments are referred to as sugar infusion and water infusion, respectively.

The sugar solutions contained 20 g of sugar in total. Assuming they would be transported throughout the tree, which has a fresh weight of 2000 g (averaged biomass), this would result in at least a 1% sugar concentration added on top of the endogenous sugars. This concentration is biologically relevant, as xylem sap typically contains < 1% sugar (Raven, 1983), whereas phloem sap has a much higher sugar concentration ranging from 15 to 30% (Esau, 2013).

The infusion started under the assumption that both tree species' C storage was depleted in the C-limited trees due to reduced leaf area. For each species, 29 C-limited and 29 nonlimited trees were randomly assigned to one of the five treatments: fast sugar infusion ($n = 6$ individuals), slow sugar infusion (6), fast water infusion (6), slow water infusion (6), and noninfusion (5). The velocity of fast infusion was 1 ml per 75 min (equivalent to 13 µl min^{-1}), and the velocity of slow infusion was roughly 1 ml per 150 min (6 µl min^{-1}). Infusion lasted up to 10 d or until all the sugar solution in the bottle was consumed. Although exact infusion rates and durations were not measured for each tree, the flow regulator ensured stable and controlled rates throughout the experiment. Periodic checks of solution depletion confirmed that infusion proceeded as expected. The same technique and setup were applied to both species to ensure consistency across treatments.

Physiological measurements and sampling

Carbon isotope composition of dark-respired CO_2 The $\delta^{13}C$ of dark-respired CO_2 ($\delta^{13}C_R$) of the tree crown shoots and the roots (+ pot soil; hereafter referred to as roots) were measured between 9 h : 18 h Central European Time (CET) during two campaigns: 1 and 4 wk after the start of the sugar infusion treatments. We used a Picarro G2131-i cavity ringdown spectroscopy isotopic-CO_2 gas analyzer (Picarro Inc., Santa Clara, CA, USA). The inlet and outlet were on the sides and bottoms of a black plastic bag. No fans were installed inside the bags because of the limited space. After selecting an inlet and an outlet of the gas analyzer, we connected them to the corresponding inlet and outlet of the bag, forming a closed loop. The black plastic bag was tightly wrapped around with a cord sealing the upper crown (shoot, including leaves and small branches), while a separate black plastic bag was used to seal the lower part (roots, including roots,

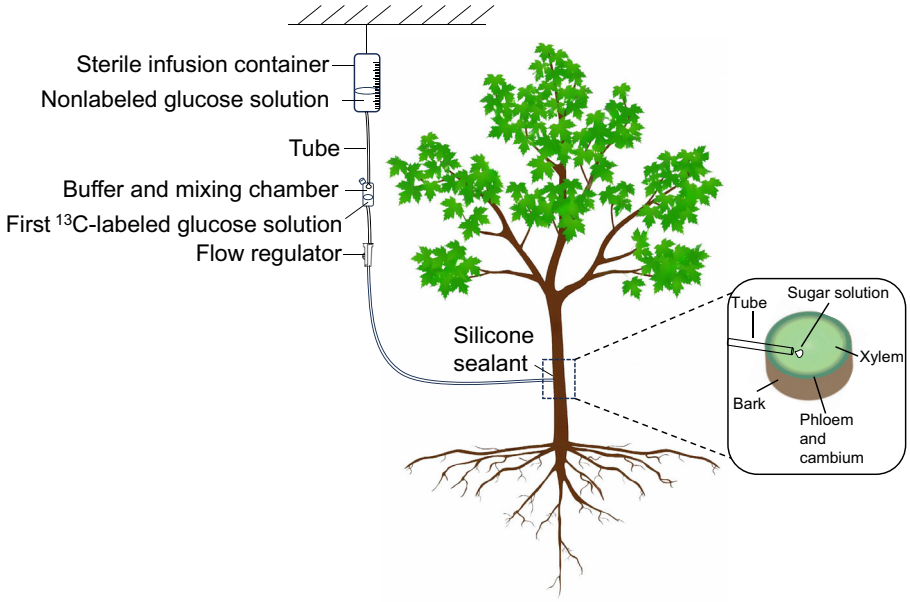

Fig. 1 Schematic representation of the sugar infusion apparatus. A nondefoliated sycamore maple tree (*Acer pseudoplatanus*) is shown as an example. To ensure the labeled sugar was taken up before the nonlabeled sugar, we first added the ^{13}C-labeled glucose solution to the buffer and mixing chamber and subsequently added the nonlabeled glucose to the sterile infusion container. The sterile infusion container holds the nonlabeled sugar solution, which flows through a tube into the buffer and mixing chamber, where a flow regulator controls the infusion rate. The solution is then delivered into the tree stem through a drilled hole reaching the xylem, with the insertion point sealed using silicone sealant to prevent leaks. Once introduced into the xylem apoplast, the sugars might be transported upward to the leaves via the transpiration stream and downward to the roots via xylem–phloem exchange. Membrane-bound sugar transporters facilitate their uptake into the symplast of leaf and root cells, where they are metabolized or respired, producing energy and labeled CO_2 that can be traced. This apparatus allows for the controlled delivery of the sugar solution into the xylem, ensuring efficient uptake and distribution throughout the tree.

and soil). The measurement lasted until the internal CO_2 concentration (*c.* 420 ppm) increased by *c.* 200 ppm (*c.* 5–15 min for the leaf and small branches and *c.* 3–5 min for the roots and soil). Three standard gases (Std1: 350 ppm for CO_2; Std2: 1350 ppm for CO_2; Std3: −9.92‰ for $\delta^{13}C$) were scanned until the values were stable enough to carry out two-point gain and offset calibrations for CO_2 measurements and single-point delta value offset calibrations for $\delta^{13}C$ measurements. The $\delta^{13}C_R$ determination of each measurement was conducted using the widely adopted Keeling plot approach (Keeling, 1961).

Foliar gas exchange Seven days after the sugar infusion treatment started, leaf photosynthetic parameters were measured using a Li-Cor 6800 infrared gas analyzer system (Li-Cor, Lincoln, NE, USA). Measurements of light-saturated assimilation rate (A_{sat}), maximum carboxylation rate (Vc_{max}), the maximum photosynthetic electron transport rate (J_{max}), the ratio of intercellular CO_2 concentration to ambient CO_2 concentration (c_i/c_a), and stomatal conductance to water vapor (g_{sw}) were carried out in the form of CO_2 response curves (A/C_i curves). One fully sun-exposed leaf from the top third of the canopy was selected from each tree. Measurements were conducted between 9 h : 16 h CET when photosynthesis was most active. Measurements of A/Ci curves were conducted using a reference CO_2 concentration, adjusted sequentially to 400, 300, 200, 100, 50, 0, 400, 400, 600, 800, 1000, 1200, 1500, and 2000 ppm, with settings of 1500 μmol m^{-2} s^{-1} light-saturating photosynthetic photon flux density and 25°C chamber temperature matching daytime ambient air temperature. The light source in the chamber consisted of a mix of 90% red light and 10% blue light. Relative air humidity was set at 60–70%, similar to the growing conditions to which the trees were acclimated when the vapor pressure deficit was *c.* 1.3 kPa. Data were collected after maintaining steady-state gas exchange rates for a minimum of 5 min. Following each measurement of pine trees, the portion of needles within the cuvette, which was smaller than the chamber (i.e. 2 cm^2), was harvested. The projected leaf area was determined with a flatbed scanner (Epson Perfection V800 Photo; Epson, Amsterdam, the Netherlands) and used to correct the leaf gas exchange data.

At 400 ppm of CO_2 concentration, A_{sat}, c_i/c_a, and g_{sw} were taken from the first point of the A/C_i curves. The Farquhar model for photosynthesis (Sharkey *et al.*, 2007) and the default fitting methods of the PLANTECOPHYS package (Duursma, 2015) were used to fit the A/C_i curves to determine Vc_{max} and J_{max}.

Dark respiration rates and dark-adapted fluorescence Following the A/Ci measurements, the Li-Cor 6800 infrared gas analyzer equipment was used to evaluate the maximum photochemical efficiency (F_v/F_m) on a neighboring leaf in accordance with the

previously outlined protocols (Didion-Gency *et al.*, 2022). Leaves were kept in darkness for adaptation using an aluminum foil for at least 30 min before the measurements. With the exception of PAR and CO_2 concentration, which were kept at 0 µmol m^{-2} s^{-1} and 400 ppm, respectively, the other parameter settings were consistent with the *A*/*Ci* curves. Dark respiration rates (R_{dark}) were taken after the dark acclimation period. A saturating pulse of bright red light (8000 µmol m^{-2} s^{-1} PAR, 1000 ms pulse width) was used to measure the initial fluorescence (F_0) and maximum fluorescence (F_m). Variable fluorescence (F_v) was computed by subtracting F_0 from F_m.

Chlorophyll concentration Seven days after the sugar infusion treatment started, the Chl content index (CCI) was measured on the same leaves used for *A*/*Ci* measurements with a Chl concentration meter (MC100; Apogee Instruments Inc., Logan, UT, USA). Chl content index was used to calculate Chl concentration (Chl, in µmol m^{-2}) based on the relationship between CCI and Chl (Parry *et al.*, 2014).

Sampling of plant tissues Eight days after infusion started, newly emerged leaves/needles were collected from each individual. Fifty-nine days after infusion started, newly (i.e. after the infusion began) emerged leaves/needles, twigs, and fine roots (< 2 mm in diameter) were collected. In May, 'newly emerged' referred to leaves/needles that developed within the first week after infusion, whereas in July, 'newly emerged' referred to leaves/needles that continued to develop over the 8 wk. We collected the roots by pulling the trees out of their pots and sampling the outermost white fine roots. Fine roots were rinsed with tap water to remove any adhering soil particles. After collection, all plant materials, including leaves/needles, twigs, and fine roots, were directly stored in the freezer at −20°C within 1 h to halt respiration. Leaves/needles, twigs, and fine roots were dried at 60°C for 72 h until a stable weight was achieved. All dried samples from the two harvests were ground to powder with a ball mill (Retsch MM 400; Retsch GmbH, Haan, Germany) for the analysis of NSC concentrations and $\delta^{13}C$ of cellulose.

Nonstructural carbohydrates The NSC concentration was determined according to previously described protocols (Schönbeck *et al.*, 2018). Ten to 12 mg of ground sample powder was extracted in 2 ml distilled water and then put in hot steam for 30 min to dissolve soluble sugars. After pipetting the extract for total NSC analysis (see description below), the supernatant was obtained for 20 min during which the solids in the solution settled down. An aliquot of 200 µl of the transferred supernatant was added to 100 µl of Invertase from baker's yeast (Sigma-Aldrich) to break down sucrose to fructose and glucose. After centrifugation at *c.* 6708 ***g*** (corresponding to 10 000 rpm for 3 min) and enzymatic conversion to gluconate-6-phosphate (hexokinase reaction with Isomerase from baker's yeast and transformation of fructose into glucose, Sigma Diagnostics, St Louis, MO, USA), the total amount of glucose (free sugars) was determined by photometric analysis at 340 nm in flat-bottom 96-well microplate photometer (HR 7000; Hamilton, Reno, NE, USA). The total amount of NSC was measured by transferring 500 µl of the extract with solid (containing sugars and starch) incubated with a fungal amyloglucosidase from *Aspergillus niger* (Sigma-Aldrich) for 15 h at 49°C to digest starch into glucose. Total NSC was determined by photometric analysis as described above. The concentration of starch was calculated as total NSC minus soluble sugars. Pure starch and glucose, fructose, and sucrose solutions were used as standards. To ensure comparability and reproducibility between runs, a standard plant powder (8.5–9.5 mg Orchard leaves; Leco, St. Joseph, MI, USA) was included in each analytical run. NSC concentrations are presented as a percentage of dry matter. All samples were prepared and analyzed within the same laboratory following standardized procedures to minimize variability, and replicate measurements showed only minor differences across runs (Landhäusser *et al.*, 2018).

α-cellulose extraction All plant materials were homogenized before cellulose extraction using a steel ball mill (Retsch MM400). Cellulose was extracted based on Gaudinski *et al.* (2005), following additional recommendations by Rani *et al.* (2023). In brief, fine powder of leaf (100 mg), twigs (30 mg), and fine roots (15 mg) was transferred into F57 fiber filter bags (Ankom Technology, Macedon, NY, USA) and heat-sealed. Lipids were removed by subjecting the sample bags to a toluene/ethanol (2 : 1) solution using a Soxhlet apparatus for at least 8 h, followed by an additional 8-h treatment with pure ethanol. Subsequently, water-soluble compounds were removed by boiling the sample bags in deionized water for 4 h, three times bleached with 7% sodium chlorite (pH 4–5, adjusted with acetic acid) in an ultrasonic bath at 60°C for a maximum of 10 h to remove lignin, and then rinsed three times with boiling deionized water, and dried for at least 4 h in a drying oven at 60°C. In a final step, α-cellulose was obtained by treating the samples with a 17% sodium hydroxide solution at room temperature in an ultrasonic bath for 1 h to remove fats, oils, tannins, and hemicellulose residues. The neutralization of sodium hydroxide was achieved by adding 96% acetic acid and several rinses with deionized water at room temperature, followed by drying the samples overnight at 60°C. The percentage of cellulose content (Cellulose %) was calculated as the ratio of the weight of extracted and dried cellulose to the initial weight of each sample. Approximately 1 mg of dry cellulose material of each sample was used for isotope analyses.

Isotope analysis and calculation Approximately 1 ± 0.1 mg of dry cellulose material was weighed into silver foil capsules (8 × 5 mm, Säntis, Rüthi, Switzerland). $\delta^{13}C$ (‰) and C concentration (C%) in the cellulose of all samples were analyzed with an elemental analyzer (IsoEarth; Sercon, Crewe, UK) and isotope ratio mass spectrometer (HS2022; Sercon) in the WSL Stable Isotope Research Centre SIRC. The $\delta^{13}C$ values were reported against Vienna Pee Dee Belemnite (VPDB) with a precision better than 0.2‰.

To calculate the amount of ^{13}C-label in cellulose (g), δ^{13}C of cellulose was converted to atom% according to Ruehr *et al.* (2009):

$$\text{atom\%} = \frac{100 \times 0.0111802 \left(\frac{\delta}{1000} + 1\right)}{1 + 0.0111802 \left(\frac{\delta}{1000} + 1\right)} \quad \text{Eqn 1}$$

where 0.0111802 is the standard value for the isotope ratio of VPDB.

^{13}C atom excess (%) was then calculated as follows:

$$^{13}\text{C atom excess} = \text{atom\%}_s - \text{atom\%}_c \quad \text{Eqn 2}$$

where atom%$_s$ is the ^{13}C atom percentage of the labeled sample, and atom%$_c$ represents the atom percentage of the unlabeled control sample (natural abundance). Finally, the following equation was used to calculate the amount of ^{13}C-label in cellulose (g):

$$^{13}\text{C} = \frac{^{13}\text{C atom excess}}{100} \times \text{Biomass} \times \text{Cellulose\%} \times \frac{\text{C\%}}{100} \quad \text{Eqn 3}$$

where Biomass (g) is the dry weight of the respective tissue.

Leaf nonstructural C residence time estimation Leaf nonstructural C residence time represents the mean duration that nonstructural C remains in a leaf under steady-state conditions. To estimate the leaf nonstructural C residence time, total leaf nonstructural C mass (TLNCM) was calculated as follows:

$$\text{TLNCM(g)} = \text{TLB(g)} \times \text{Leaf NSC concentration(\%)} \times \text{C Fraction} \quad \text{Eqn 4}$$

where TLB is the estimated total leaf biomass, and the C Fraction (i.e. the mass fraction of C in nonstructural carbohydrates) in NSC is *c.* 40%.

Daily carbon (C) gain was calculated as the sum of endogenous (endo) C gain and exogenous (exo) C gain in leaves, minus night-respired C. These components were estimated using the following equations developed on the basis of Asao *et al.* (2025):

$$\text{Endo C gain (g)} = \frac{A_{sat} \times (\text{D} \times 90\%)}{\text{LMA}} \times \text{TLB} \times \frac{12}{10^6} \quad \text{Eqn 5}$$

$$\text{Night respired C (g)} = \frac{R_{dark} \times (24 - \text{D})}{\text{LMA}} \times \text{TLB} \times \frac{12}{10^6} \quad \text{Eqn 6}$$

where A_{sat} (μmol CO_2 m^{-2} s^{-1}) and R_{dark} (μmol CO_2 m^{-2} s^{-1}) were converted to grams using leaf mass per area (LMA) and daylight duration (D). LMA values were based on Forrester *et al.* (2017), with estimates of 37 g m^{-2} for *A. pseudoplatanus* and 250 g m^{-2} for *P. sylvestris*, assuming no differences among treatments due to the short duration between the start of the experiment and the first sampling. Daylight duration was defined as the period from sunrise to sunset on 27 May 2023 (7 d after the infusion began), adjusted to 90% to account for reduced light availability at dawn and dusk (Asao *et al.*, 2025). In Eqns 5 and 6, the molar mass of C (12 g mol^{-1}) was used, and values in μmol were converted to mol by dividing by 10^6.

$$\text{Exo C gain in leaves(g)} = \text{TLNCM}_{diff} + \text{Endo C gain}_{diff} + \text{Night respired C}_{diff,} \quad \text{Eqn 7}$$

$$\text{Daily C gain}\left(\text{g d}^{-1}\right) = \text{Endo C gain} + \text{Exo C gain} - \text{Night respired C} \quad \text{Eqn 8}$$

TLNCM_{diff} (g) was calculated as the TLNCM (g) of sugar-infused trees minus that of control trees. Endo C gain_{diff} (g) was calculated as the Endo C gain (g) of control trees minus that of sugar-infused trees, to account for potential negative effects on photosynthesis. Night-respired C_{diff} (g) was calculated as the Night-respired C (g) of sugar-infused trees minus that of control trees.

Finally, the following equation was used to calculate leaf nonstructural C residence time, which was defined as the ratio of total leaf nonstructural C biomass to potential daily C gain. This approach assumes that mature leaves operate near a daily steady state such that average C gain is balanced by respiratory and export losses (Smith & Stitt, 2007; Graf *et al.*, 2010; Asao *et al.*, 2025). Under this assumption, a higher NSC concentration implies a longer residence time, and hence, a lower relative rate of export. In situations where the steady-state assumption does not fully hold, such as under defoliation or sugar infusion, the calculated values were interpreted as approximations of C dynamics.

$$\text{Leaf nonstructural C residence time(day)} = \frac{\text{TLNCM(g)}}{\text{Daily C gain}\left(\text{g d}^{-1}\right)}. \quad \text{Eqn 9}$$

Statistical analysis

Statistical analyses were performed using R v.4.4.0 (R Core Team, 2024). The effects of species, defoliation, and infusion treatments on leaf photosynthetic parameters (A_{sat}, Chl, Vc_{max}, J_{max}, g_{sw}, c_i/c_a, and F_v/F_m), $\delta^{13}C_R$, tissue NSC (sugar, starch, and NSC) concentrations, and δ^{13}Cc values were determined through linear mixed-effects models using the R package LME4 (Bates *et al.*, 2024). There were no significant differences in these parameters between water infusion treatments and noninfused controls (Table S1), and thus data collected from water infusion were not included in further analyses. Species (maple vs pine), sugar infusion treatment (noninfusion vs slow sugar infusion vs fast sugar infusion), and defoliation treatment (C-limited vs non-C-limited) were used as fixed effects in the models, and the individual tree was included as a random

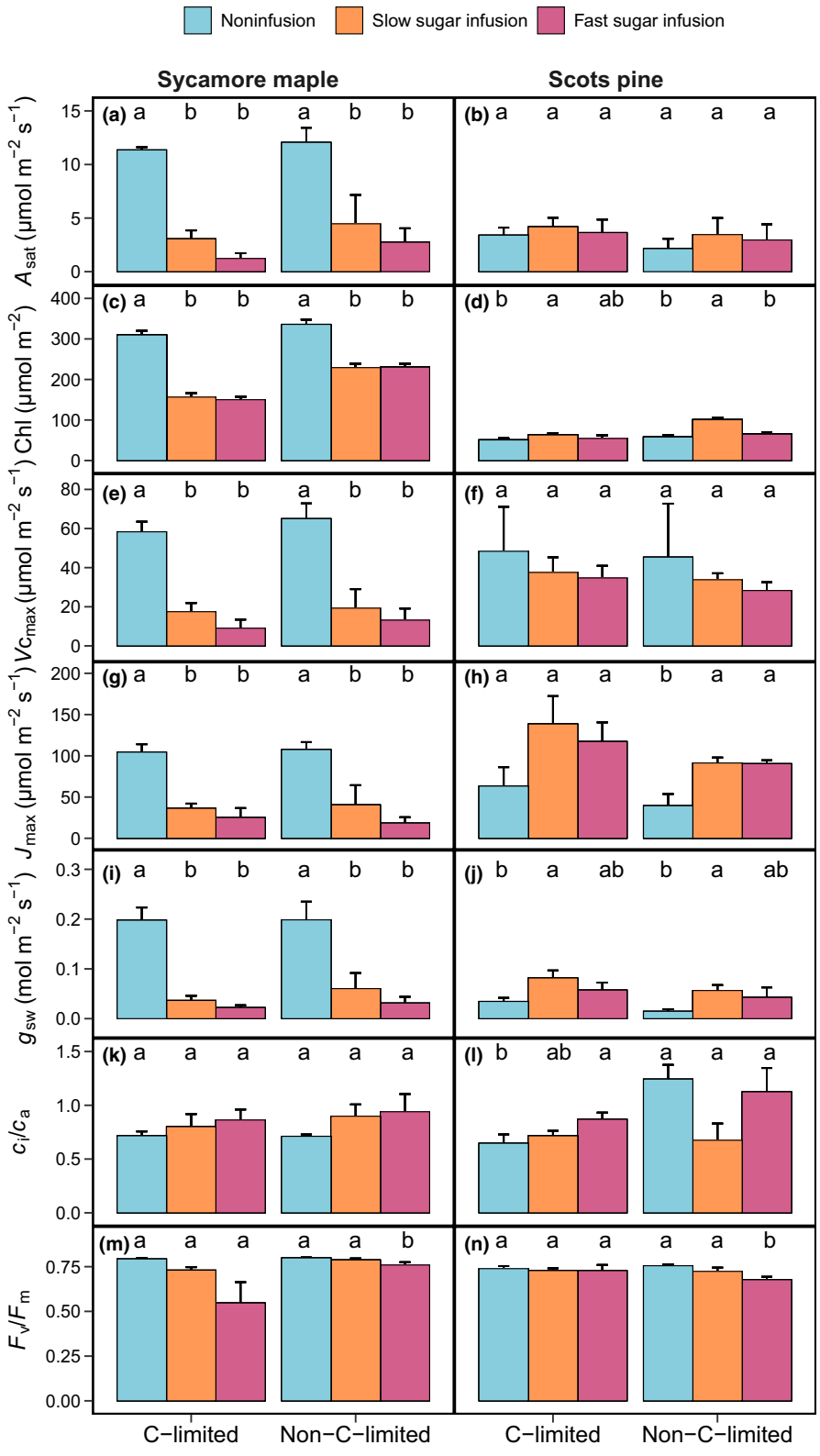

Fig. 2 Leaf gas-exchange, pigment, and fluorescence responses to sugar infusion treatment. Light-saturated assimilation rate (A_{sat}, a, b), Chl concentration (Chl, c, d), maximum velocity of carboxylation (Vc_{max}, e, f), maximum photosynthetic electron transport rate (J_{max}, g, h), stomatal conductance to water vapor (g_{sw}, i, j), the ratio of intercellular CO_2 concentration to ambient CO_2 concentration (c_i/c_a, k, l), and maximum photochemical efficiency (F_v/F_m, m, n) are shown for maple (*Acer pseudoplatanus*) and pine (*Pinus sylvestris*) trees 1 wk after the start of sugar infusion. C-limited, defoliated trees; non-C-limited, nondefoliated trees; noninfusion (control trees, blue, $n = 5$ trees), slow sugar infusion (orange, $n = 6$), and fast sugar infusion (pink, $n = 6$) with ^{13}C-labeled glucose solution. Mean values and error bars indicating + SE are shown. Different lowercase letters indicate significant differences among infusion treatments (i.e. noninfusion, slow sugar infusion, and fast sugar infusion) within each defoliation treatment for each species (ANOVA followed by a Duncan's *post hoc* test: $P \leq 0.05$).

effect. The Shapiro–Wilk test was used to test normality. In the final models, the dependent variables were log- or square root-transformed to achieve normality and homoscedasticity of the residuals. ANOVA, followed by Duncan's *post hoc* tests, was performed to evaluate the differences between species, defoliation treatment, and sugar infusion treatment.

New Phytologist

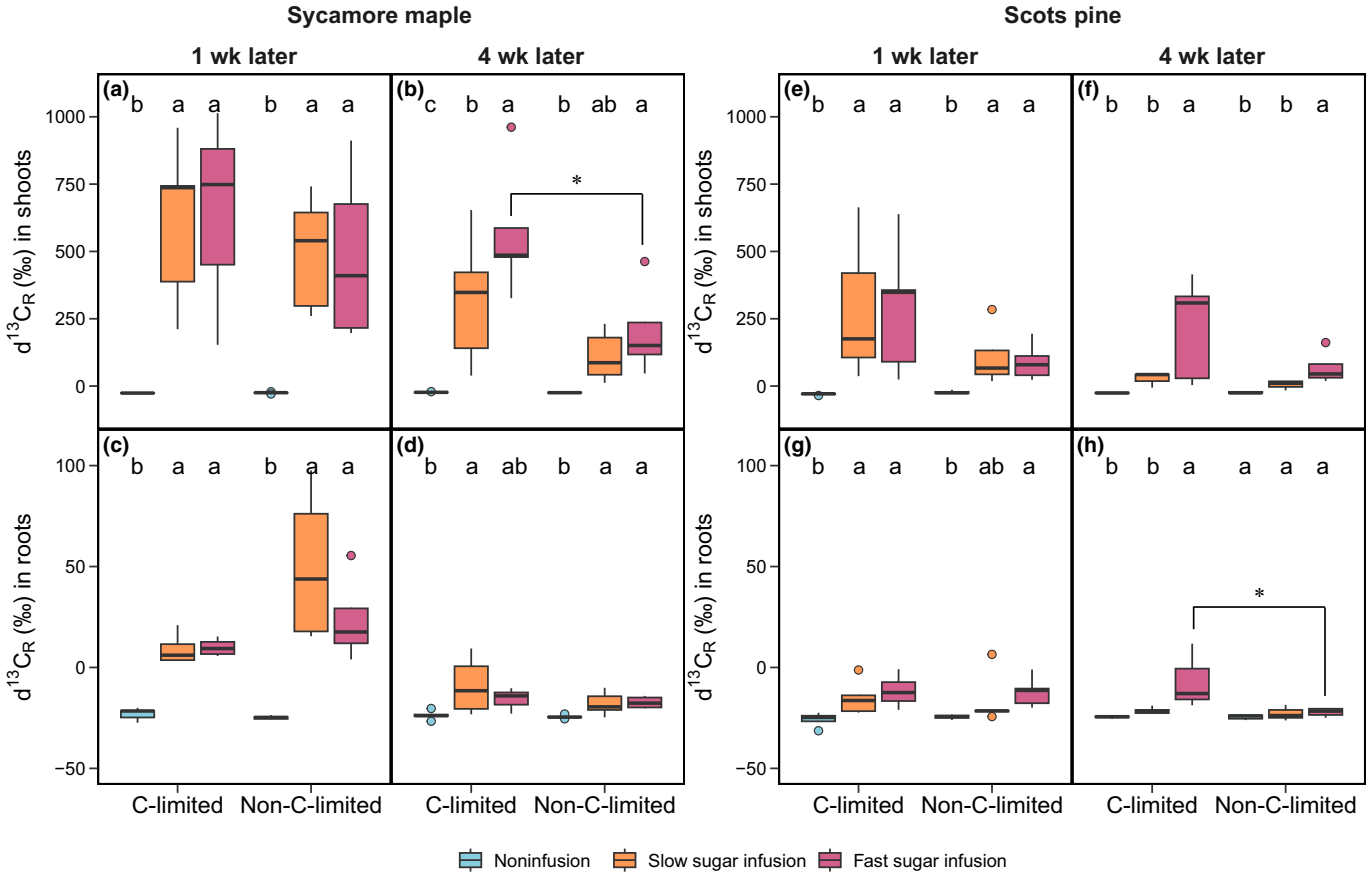

Fig. 3 ^{13}C enrichment in plant-respired CO_2 in response to sugar infusion, defoliation, and species. Carbon isotopic composition of dark-respired CO_2 ($\delta^{13}C_R$) is shown for maple (*Acer pseudoplatanus*) and pine (*Pinus sylvestris*) crown shoots (a, b, e, f) and roots (c, d, g, h) at 1 wk (a, c, e, g) and 4 wk (b, d, f, h) after the start of sugar infusion. C-limited, defoliated trees; non-C-limited, nondefoliated trees; noninfusion (control trees, blue, $n = 5$ trees), slow sugar infusion (orange, $n = 6$), and fast sugar infusion (pink, $n = 6$) with ^{13}C-labeled glucose solution. The boxes represent the first quartile, median, and third quartile, while the whiskers indicate 1.5 times the interquartile range in both directions. The dots represent measurements outside the whisker range. Different lowercase letters indicate significant differences among infusion treatments (i.e. noninfusion, slow sugar infusion, and fast sugar infusion) within each defoliation treatment for each species (ANOVA followed by a Duncan's *post hoc* test; $P \leq 0.05$). An asterisk indicates significant differences between defoliation treatment within each sugar infusion treatment and campaign for each species (*, $0.01 \leq P \leq 0.05$).

The relationships between leaf NSC concentration (sampled 8 d after the infusion started in May) and leaf photosynthetic parameters (A_{sat}, Chl, Vc_{max}, J_{max}, g_{sw}, c_i/c_a, and F_v/F_m) were analyzed across all treatments and for each species using the R package GGPMISC (Aphalo, 2021).

We generated the graphs using the R package GGPLOT2 (Wickham, 2016) and created the final assembly of the graphs using the R package PATCHWORK (Pedersen, 2022).

Results

Photosynthetic parameters and ^{13}C-label in dark respiration

One week after the infusions started, they significantly affected photosynthetic parameters in maple and pine, but the responses varied between species and C limitation conditions (Table S2). Compared to the noninfused control, maple trees – exposed to both the slow and fast sugar infusion – significantly reduced A_{sat}, Chl, Vc_{max}, J_{max}, and g_{sw}. This reduction was observed in C-limited and non-C-limited maple trees (all $P < 0.05$; Fig. 2a,c,e,g,i). In non-C-limited maple and pine trees, F_v/F_m significantly decreased under fast sugar infusion ($P < 0.05$; Fig. 2m,n). By contrast, neither slow nor fast sugar infusion affected A_{sat} or Vc_{max} in pine (Fig. 2b,f). However, slow sugar infusion significantly increased Chl and g_{sw} in both C-limited and non-C-limited pine trees ($P < 0.01$; Fig. 2d,j). Additionally, in non-C-limited pine, J_{max} increased significantly after both slow and fast sugar infusion ($P < 0.01$; Fig. 2h). Under C-limited conditions, c_i/c_a significantly increased in pine following fast sugar infusion ($P < 0.05$; Fig. 2l).

Comparing C-limited and non-C-limited trees, Chl was significantly lower in C-limited maple under both slow and fast sugar infusion ($P < 0.001$; Fig. 2c; Table S3). A similar trend was observed in pine under slow sugar infusion ($P < 0.001$; Fig. 2d; Table S3). In noninfused pine trees, g_{sw} was significantly higher in C-limited than in non-C-limited trees ($P < 0.05$; Fig. 2j;

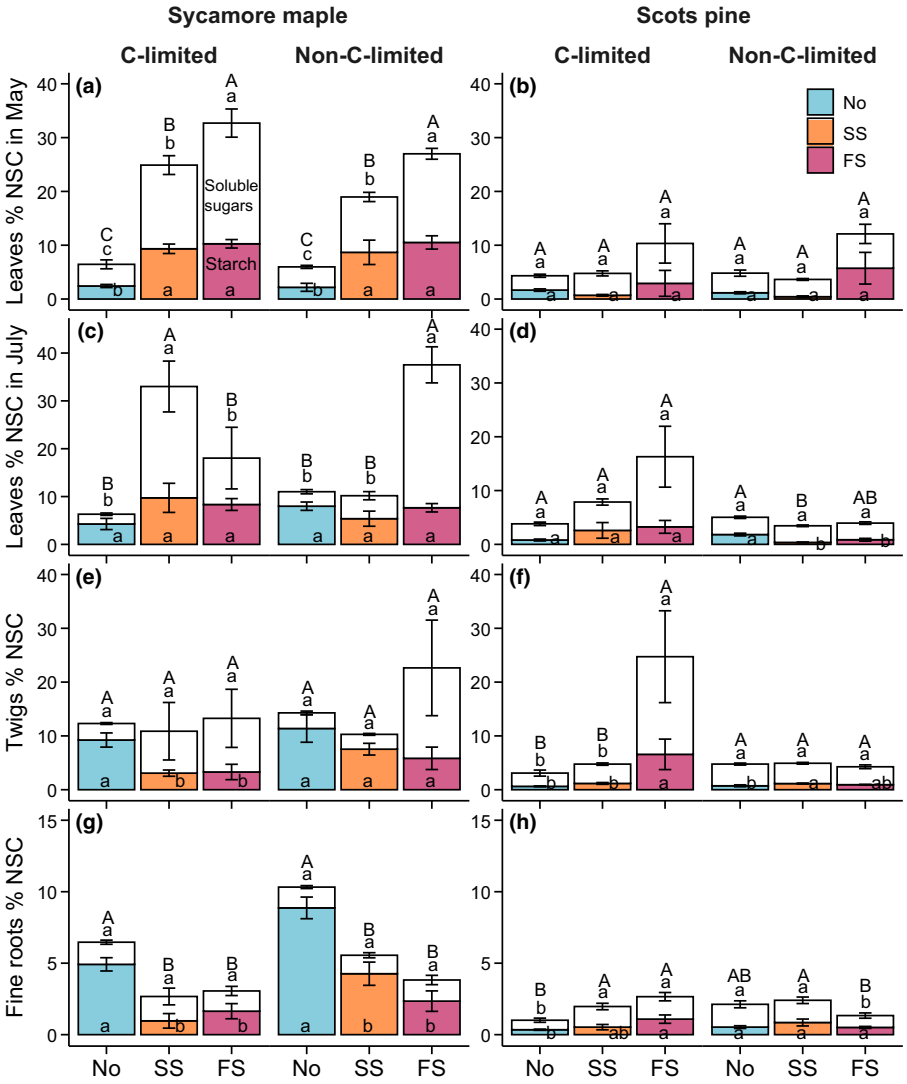

Fig. 4 Nonstructural carbohydrate responses (NSC, mean ± 1 SE) to sugar infusion, defoliation, and species. Tissue NSC concentrations, separated into soluble sugars (upper white parts) and starch (lower colored parts) are shown for maple (*Acer pseudoplatanus*) and pine (*Pinus sylvestris*) trees. Samples were taken 8 d (a, b) and 59 d (c – h) after the start of sugar infusion. C-limited, defoliated trees; non-C-limited, nondefoliated trees; noninfusion (control trees, $n = 5$ trees), slow ($n = 6$), and fast infusion ($n = 6$) with ^{13}C-labeled glucose solution. Different lowercase letters indicate significant differences in sugars (upper letters) and starch (lower row, within the colored bars) among infusion treatments (i.e. noninfusion (No, blue), slow sugar infusion (SS, orange), and fast sugar infusion (FS, pink)) within each defoliation treatment for each species (ANOVA followed by a Duncan's *post hoc* test; $P \leq 0.05$). Different uppercase letters indicate significant differences in total NSC concentrations among infusion treatments within each defoliation treatment for each species ($P \leq 0.05$).

Table S3), whereas c_i/c_a showed the opposite trend ($P < 0.01$; Fig. 2l; Table S3). Higher g_{sw} allows more CO_2 to enter the needles, but the lower c_i suggests higher CO_2 assimilation, indicating a higher demand for CO_2. This pattern suggests that C-limited trees are actively drawing down CO_2 to compensate for their C deficit.

One week after the infusions started, the ^{13}C signals in dark-respired CO_2 ($\delta^{13}C_R$) from both shoots and roots (+ pot soil) were significantly increased by the sugar infusion ($P < 0.001$; Table S2), and there were interactions between species and infusion treatment ($P < 0.05$; Table S2). Compared to the noninfused control trees, slow and fast sugar infusion significantly increased the ^{13}C signal in both shoot- and root-respired CO_2 in either C-limited or non-C-limited trees for the two species ($P < 0.05$; Fig. 3a,c,e,g). Four weeks after the infusion started (Table S2), the exogenous sugars still affected the $\delta^{13}C_R$ signal in both shoot- and root-respired CO_2 in C-limited and non-C-limited maple trees ($P < 0.05$; Fig. 3b,d). By contrast, only the fast sugar infusion significantly affected the root $\delta^{13}C_R$ signal in pines after 4 wk and only in C-limited pine trees ($P < 0.05$; Fig. 3f,h). The root $\delta^{13}C_R$ signal was significantly higher in C-limited pines than in non-C-limited pines ($P < 0.05$; Fig. 3h; Table S3).

Soluble nonstructural carbohydrate concentrations

Eight days after infusion started, noninfused trees showed no significant differences in NSC concentrations between C-limited and non-C-limited trees in both species (Fig. 4a,b; Table S3). However, in noninfused maple trees, leaf nonstructural C residence time was significantly shorter in C-limited than in non-C-limited trees ($P < 0.01$; Fig. S3; Table S3). By July, 59 d after sugar infusion started, noninfused C-limited trees in both species showed lower starch or total NSC (TNSC) concentrations in leaves and fine roots, indicating C limitation (all $P < 0.05$; Fig. 4c,d,g,h; Table S3).

One week after sugar infusion in May, both infusion treatments increased maple leaf TNSC concentrations three to five

times (all $P < 0.05$; Fig. 4a; Table S2), accompanied by leaf senescence (Fig. S4). However, no such increase or senescence was observed in pine needles (Figs 4b, S4).

Fifty-nine days after sugar infusion started in July, C-limited sugar-infused maple trees retained high leaf TNSC concentrations (Fig. 4c), but starch in twigs decreased by two-thirds

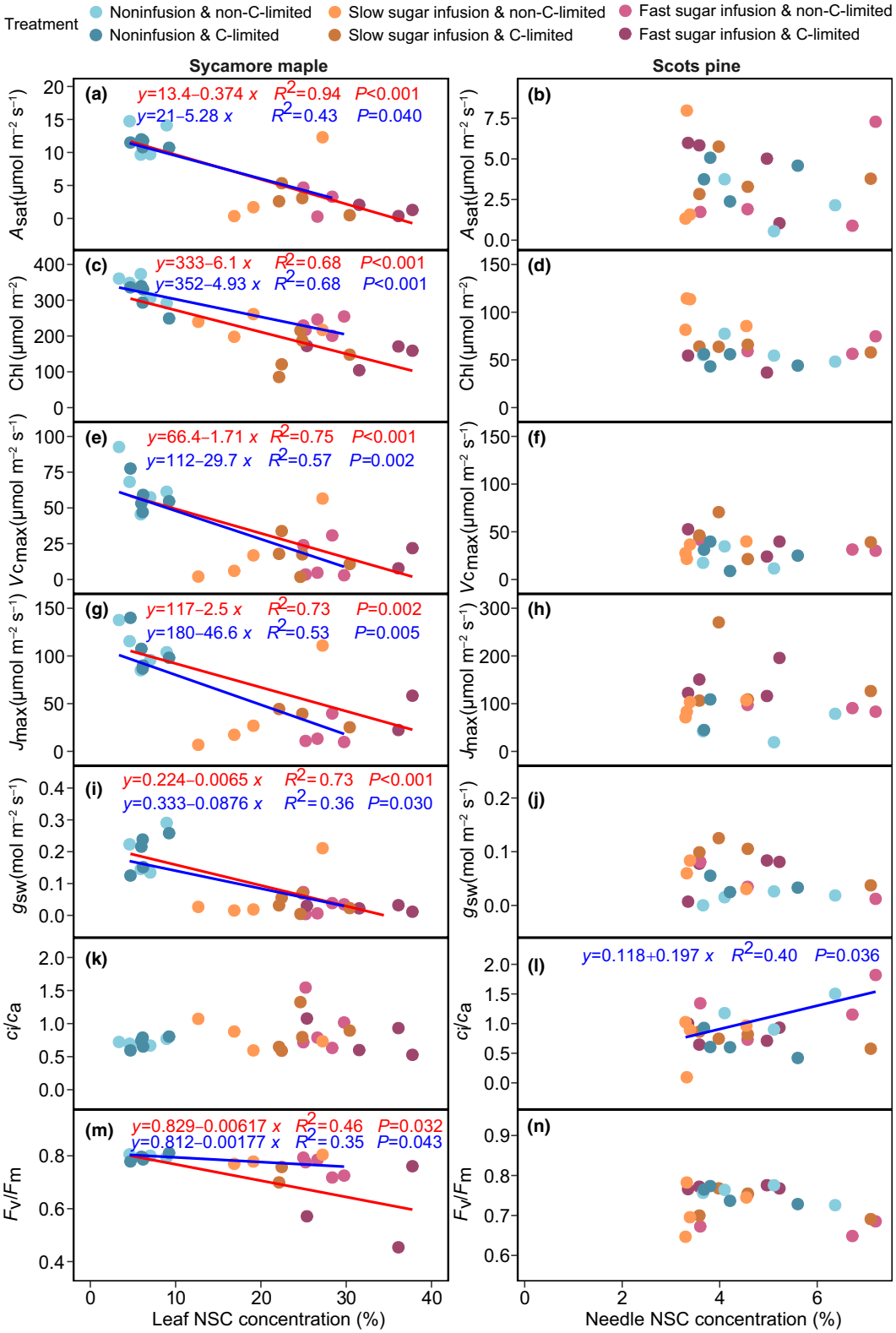

Fig. 5 Relationships between leaf-gas exchange and leaf/needle NSC concentrations 1 wk after the start of sugar infusion. Linear regression analysis of nonstructural concentration (NSC) of leaves/needles is shown in relation to: light-saturated assimilation rate (A_{sat}, a, b), Chl concentration (Chl, c, d), maximum velocity of carboxylation (Vc_{max}, e, f), maximum photosynthetic electron transport rate (J_{max}, g, h), stomatal conductance to water vapor (g_{sw}, i, j), the ratio of intercellular CO_2 concentration to ambient CO_2 concentration (c_i/c_a, k, l), and maximum photochemical efficiency (F_v/F_m, m, n) of maple (*Acer pseudoplatanus*) and pine (*Pinus sylvestris*) trees. C-limited, defoliated trees; non-C-limited, nondefoliated trees; noninfusion (control trees, $n = 5$ trees), slow ($n = 6$), and fast infusion ($n = 6$) with ^{13}C-labeled glucose solution. Colored lines indicate significant correlations within the corresponding defoliation treatments (blue for nonlimited and red for C-limited). When the linear regression was significant, the linear model equation, the coefficients of determination (R^2), the *P*-value, and the regression line are given. Analyses were done with all defoliation and sugar infusion treatments pooled (bright-blue, noninfusion and non-C-limited; dark-blue, noninfusion and C-limited; bright-orange, slow sugar infusion and non-C-limited; dark-orange, slow sugar infusion and C-limited; bright-pink, fast sugar infusion and non-C-limited; dark-pink, fast sugar infusion and C-limited).

($P < 0.01$; Fig. 4e), compared to noninfused maple. Starch and TNSC in fine roots declined in both C-limited and non-C-limited trees ($P < 0.01$; Fig. 4g). By contrast, pine needles showed no NSC accumulation (Fig. 4d). NSC concentrations in fine roots of C-limited pines increased with sugar infusion ($P < 0.05$), raising them to levels similar to those of non-C-limited trees (Fig. 4h).

Relationships between leaf/needle NSC level and photosynthetic parameters

Leaf NSC concentrations were significantly negatively related to the photosynthetic parameters in both C-limited and non-C-limited maple trees (Fig. 5), except for c_i/c_a (Fig. 5k). By contrast, no relationships existed for pine trees except for c_i/c_a in non-C-limited pines, where a positive correlation was observed (Fig. 5i).

^{13}C-label in cellulose as an indicator of structural growth

One week after sugar infusion began, it significantly increased δ^{13}C values in leaf cellulose (δ^{13}Cc) in both C-limited and non-C-limited trees of the two species (Fig. 6a,b; Table S2). Eight weeks after sugar infusion started, δ^{13}Cc values in leaves/needles, twigs, and roots were still significantly affected by infusion (all $P < 0.001$; Table S2), and species interacted with infusion treatment to significantly influence the δ^{13}Cc in roots (Table S2). Compared to the nontreated control trees, both slow and fast sugar infusion tended to increase the tissue ^{13}Cc in both C-limited and non-C-limited trees for the two species (Fig. 6), with an exception for non-C-limited pine roots (Fig. 6h). Eight weeks after sugar infusion started, under fast sugar infusion, C-limited maple trees showed significantly higher ^{13}Cc allocation to twigs, whereas C-limited pine trees allocated significantly more ^{13}Cc to fine roots, than non-C-limited trees (both $P < 0.05$; Fig. 7; Tables S3, S4).

Discussion

Effective C limitation treatments

C limitation is a crucial factor influencing tree survival (McDowell *et al.*, 2008, 2022; Anderegg *et al.*, 2015; Barker Plotkin *et al.*, 2021). In this study, we simulated C limitation by defoliating developed leaves in maple and pine, assuming the treatments effectively induced C limitation. This assumption was confirmed by significant differences observed in May (8 d after sugar infusion started) between C-limited and non-C-limited noninfused trees. In maple trees, these differences were evident in shorter leaf nonstructural C residence time (Fig. S3; Table S3). In pine trees, differences were observed in g_{sw}, c_i/c_a, and needle δ^{13}Cc values (Figs 2j,l, 6; Table S3).

Contrary to previous findings that suggest C limitation may upregulate photosynthesis to compensate for the lost leaf area (Eyles *et al.*, 2009; Pinkard *et al.*, 2011) due to an elevated C sink : source ratio (Eyles *et al.*, 2013) or alter leaf NSC levels (Wiley & Helliker, 2012; Weber *et al.*, 2019), our study found no significant differences in photosynthesis or leaf NSC levels between noninfused C-limited and non-C-limited maple trees 8 d after sugar infusion started in May (Figs 2a,b, 4a,b). One possible explanation is that trees prioritize belowground over aboveground investment when under C stress (Hagedorn *et al.*, 2016; Schönbeck *et al.*, 2020). The lack of changes in leaf NSC concentrations may also reflect the tendency for C depletion to occur in belowground tissues rather than in leaves (W. Li *et al.*, 2018; Joseph *et al.*, 2020). By May, as our analysis only focused on leaf NSC concentrations to avoid disturbing the roots, any NSC depletion in fine roots of C-limited maple trees may have already taken place. This belowground C limitation likely drove the export of NSC from leaves, resulting in shorter leaf nonstructural C residence time (Fig. S3; Table S3), supporting the effectiveness of the C limitation treatment in maple.

In noninfused pine trees, the lower c_i/c_a observed in C-limited pines suggests reduced intercellular CO_2 levels, likely due to the higher CO_2 drawdown through photosynthesis (Fig. 2l; Table S3). This interpretation is supported by significantly higher g_{sw} (and thus a higher potential for CO_2 diffusion into the needle; Fig. 2j; Table S3) and the trend toward higher A_{sat}, Vc_{max}, and J_{max} in C-limited pines, although the difference was not statistically significant (Fig. 2b,f,h; Table S3). The lower δ^{13}Cc values in May needles of C-limited pines (Fig. 6b) reflect greater discrimination against $^{13}CO_2$, consistent with increased long-term CO_2 uptake during photosynthesis (Fig. 2b). The time integration of gas exchange as provided by needle δ^{13}Cc (see Fotelli *et al.*, 2003) might better reflect photosynthesis as affected by C limitation than one-point gas exchange measurement. Together, these results demonstrate that our C limitation treatment effectively restricted C availability in both maple and pine, enabling us to study their physiological responses to sugar infusion.

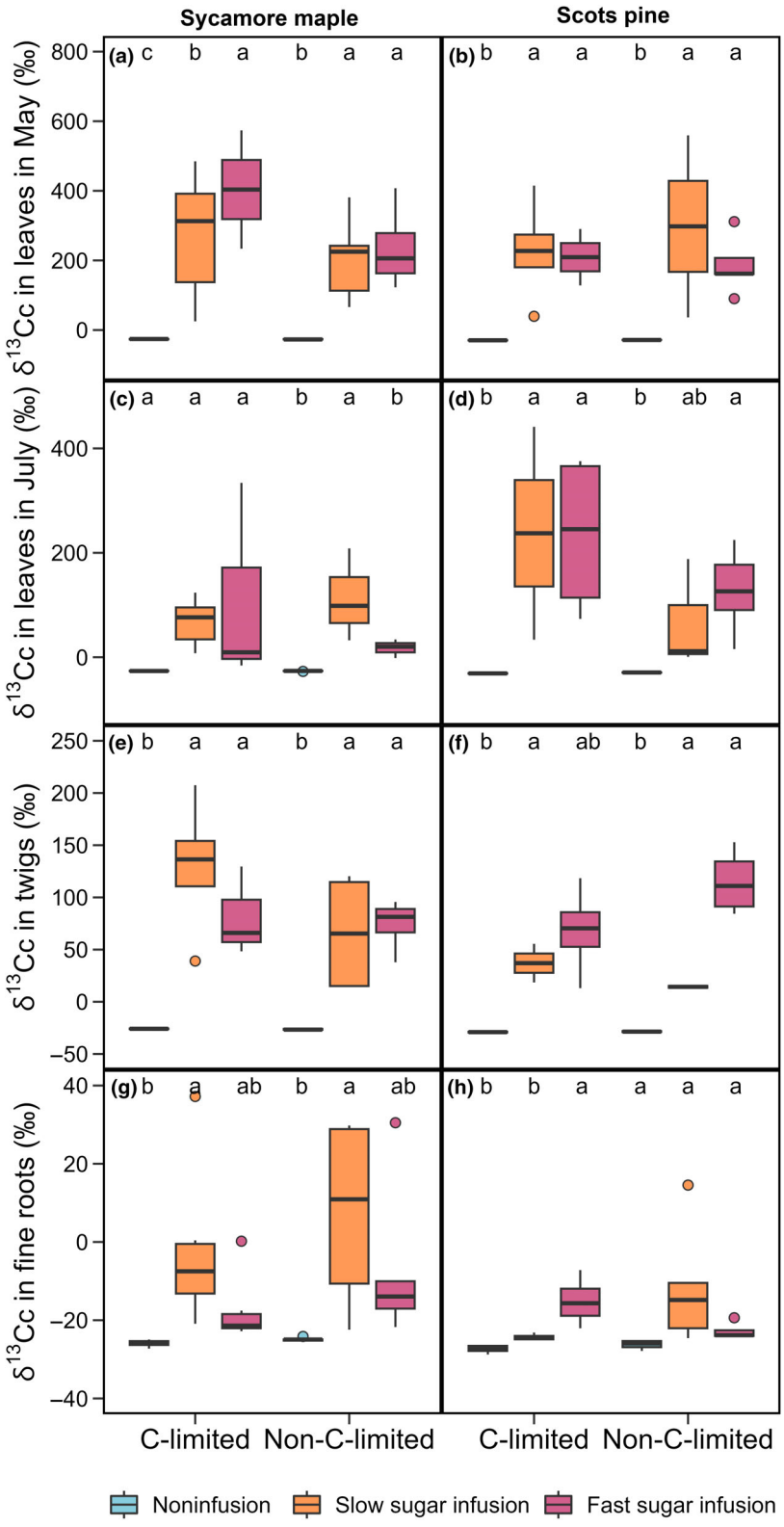

Fig. 6 ^{13}C enrichment in cellulose in response to sugar infusion, defoliation, and species. Cellulose δ^{13}Cc is shown for maple (*Acer pseudoplatanus*) and pine (*Pinus sylvestris*) trees. Samples were taken 8 d (a, b) and 59 d (c–h) after the start of sugar infusion. C-limited, defoliated trees; non-C-limited, nondefoliated trees; noninfusion (control trees, blue, $n = 5$ trees), slow sugar infusion (orange, $n = 6$), and fast sugar infusion (pink, $n = 6$) with ^{13}C-labeled glucose solution. The boxes represent the first quartile, median, and third quartile, while the whiskers indicate 1.5 times the interquartile range in both directions. The dots represent measurements outside the whisker range. Different lowercase letters indicate significant differences among infusion treatments (i.e. noninfusion, slow sugar infusion, and fast sugar infusion) within each defoliation treatment for each species (ANOVA followed by a Duncan's *post hoc* test; $P \leq 0.05$).

Negative feedback on photosynthesis in maple but not in pine after sugar infusion

Sugar infusion treatments increased leaf NSC concentrations, downregulated photosynthesis, and induced senescence in maple but not in pine trees (Figs 2, 4, S4), supporting our first hypothesis. Transport from infusion sites might occur directly via the xylem as sugars are known to be xylem mobile (Heizmann *et al.*, 2001), or might be transferred from the xylem to the phloem (Van Bel, 1990), which might, however, strongly

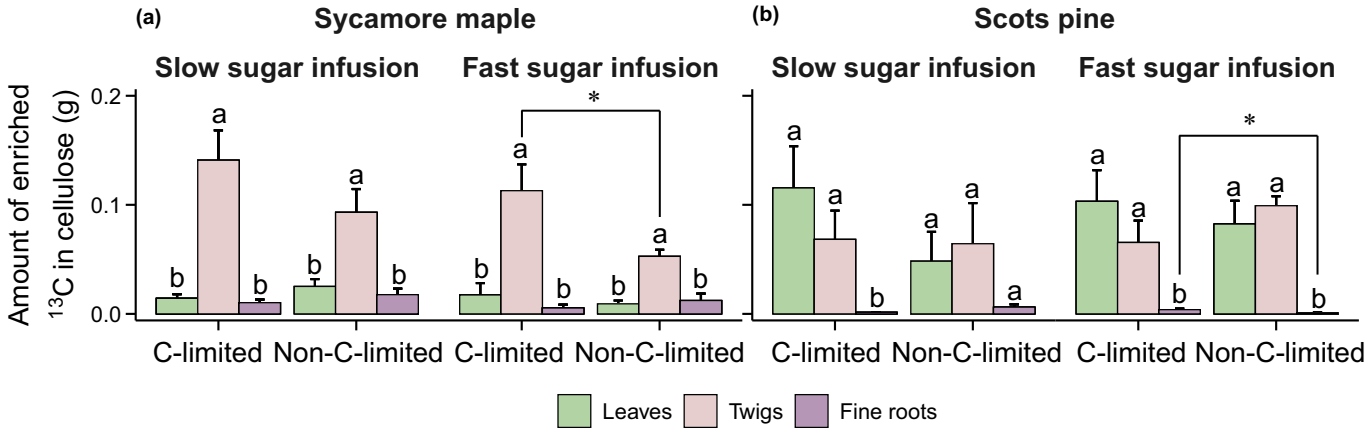

Fig. 7 The amount (g) of ^{13}C-label in cellulose in leaves/needles, twigs, and fine roots (all sampled 59 d after the start of sugar infusion) of (a) maple (*Acer pseudoplatanus*) and (b) pine (*Pinus sylvestris*) trees after slow and fast sugar infusion with ^{13}C-labeled glucose. This result quantifies exogenous C allocation to structural biomass across tissues. C-limited, defoliated trees; non-C-limited, nondefoliated trees; leaves/needles (green, $n = 6$), twigs (pink, $n = 6$), and fine roots (purple, $n = 6$) with ^{13}C-labeled glucose solution. Mean values and error bars indicating + SE are shown. Different lowercase letters indicate significant differences among tissues (i.e. leaves/needles, twigs, and fine roots) within each defoliation treatment for each species (ANOVA followed by a Duncan's *post hoc* test; $P \leq 0.05$). An asterisk indicates significant differences between defoliation treatment within each sugar infusion treatment and tissue for each species (*, $0.01 \leq P \leq 0.05$).

interfere with the normal source-to-sink transport in the tissue. Species-specific differences likely stem from wood anatomical and functional differences in the vascular and parenchyma structure of angiosperms and conifers. Maple, a diffuse-porous hardwood, has a higher proportion of parenchyma, including both ray and axial parenchyma, facilitating sugar transport within the wood (Plavcová & Jansen, 2015). This could lead to a high amount of infused sugar transported to leaves (Fig. S5a). Additionally, the significant decrease in g_{sw} observed in maple but not in pine (Fig. 2i,j) suggests that the decline in photosynthesis may have been partly driven by osmotic or hydraulic changes resulting from elevated sugar concentrations in the xylem sap. In comparison, pine, a softwood with a simpler tracheid-based vascular system and minimal axial parenchyma (Plavcová & Jansen, 2015), may exhibit less efficient transport of added sugars to its needles, which could explain why fast sugar infusion did not significantly increase NSC levels in either C-limited or non-C-limited pines. Moreover, pine photosynthesis remained unaffected (Figs 2b, 4b), supporting our second hypothesis. In pine needles, the endodermis with Casparian strips forms a boundary around the vascular and transfusion tissues (Esau, 1977). This anatomical barrier restricts the apoplastic movement of solutes, including sugars, between the vascular tissue and the surrounding mesophyll (Wu *et al.*, 2005). Consequently, radial transport of sugars is constrained, potentially limiting sugar accumulation in the photosynthetically active mesophyll. The amount of infused sugar transported to pine needles was considerably lower than that transported to maple leaves (Figs S5, S6). As a result, mesophyll sugar concentrations may not have reached the threshold to trigger photosynthetic downregulation, as outlined in the Introduction section.

In addition to structural differences, leaf longevity and resource allocation strategies may also explain these species-specific responses. Pine needles, being long-lived and persisting through winter, are adapted to store and gradually utilize sugars and starch over an extended period. This strategy helps maintain a stable C economy (Landhäusser & Lieffers, 2012). Consequently, pine might be more adjusted to varying sugar concentrations and thus less susceptible to sugar-driven photosynthetic downregulation. By contrast, maple leaves are short-lived and senesce within a single growing season. This shorter lifespan may lead to the observed rapid sugar buildup, which acts as a signal to downregulate photosynthesis and initiate early senescence. This explanation aligns with that of Zhang *et al.* (2020), who observed that deciduous broadleaf species exhibited stronger responses to excess resource availability, such as high soil nutrients and light, than evergreen conifers.

Source–sink regulatory network

Our sugar infusion experiment demonstrates that elevated exogenous C source supported respiration and growth in both maple and pine (Figs 3, 6, 7). In maple, the observed negative relationship between photosynthesis and leaf TNSC concentrations, and early senescence (Figs 5, S4), indicates a sink-driven regulatory mechanism (Gessler & Zweifel, 2024). When sink organs reach C saturation, photosynthetic activity decreases due to biochemical constraints (e.g. reduced Chl, Vc_{max}, and J_{max}; Fig. 2a,c,e,g), nutrient remobilization, and feedback inhibition (Sade *et al.*, 2018; Kumar *et al.*, 2019). Our observation also aligns with studies showing that elevated source strength, driven by increased CO_2 (Miller *et al.*, 1997) and extended growing seasons (Zani *et al.*, 2020), could induce early senescence. Supporting this mechanism, exogenous sucrose has been shown to downregulate RuBisCO and inhibit photosynthesis in sugarcane (Lobo *et al.*, 2015). Similarly, in a red maple stem chilling experiment,

an increase in leaf NSC concentration led to declined Vc_{max} and J_{max} (Rademacher *et al.*, 2022). Some studies specifically highlight hexose as a key modulator of photosynthetic activity (McCormick *et al.*, 2008; Tian *et al.*, 2024). Downregulation of photosynthetic activity also helps adjust the source–sink relationship, preventing excessive carbohydrate accumulation, as seen in citrus trees (Nebauer *et al.*, 2011). In our study, sugar accumulation also decreased g_{sw} in maple (Fig. 2i), consistent with the findings of Nebauer *et al.* (2011), who observed reduced g_{sw} along with photosynthetic downregulation in girdling experiments disrupting phloem transport. However, some studies suggest that the decline in photosynthesis induced by sugar levels is unrelated to changes in g_{sw} (McCormick *et al.*, 2008), pointing to nonstomatal limitations that may play a more significant role in photosynthetic regulation. The inconsistencies among studies may reflect differences in the plant species and experimental conditions.

After leaf senescence in maple, a second flush of new leaves emerged. This shift to new leaf growth (Fig. 7a) marked a transition from sink-driven back to source-driven control, as maple began actively producing C rather than relying only on stored reserves (i.e. starch depletion in fine roots (Fig. 4g)). In contrast to maple, pine maintained stable photosynthetic activity and showed little signs of senescence. Sugar infusion increased g_{sw} (Fig. 2j), likely as a result of osmotic adjustments in pine. Infused sugars may have increased osmotic potential in guard cells, promoting stomatal opening and thus increasing g_{sw}. However, this response may not necessarily reflect increased water uptake or loss, but rather a shift in stomatal regulation linked to sugar signaling. Furthermore, the elevated J_{max} (Fig. 2h) may suggest that pine's electron transport chain likely operates more efficiently under sugar supplementation, potentially due to the additional C supporting protein synthesis and maintenance of electron transport components. Modulating stomatal conductance and supporting its photosynthetic electron transport chain allows pine to improve C uptake and C availability for the sink tissues, ensuring efficient resource management and long-term C balance (Farquhar *et al.*, 1980; Paul & Foyer, 2001). Pine allocated exogenous C to needles and twigs (Fig. 7b; Table S4), suggesting higher leaf construction costs (Eamus & Prichard, 1998). This investment in needles reflects the evergreen strategy of maintaining functional foliage year-round to ensure continuous C assimilation. Higher C allocation to twigs may serve as an adaptive strategy to support branch growth and reserves during the growing season. Evergreen species store C in branches for new spring growth (Palacio *et al.*, 2018), underscoring their ecological strategies for managing C resources efficiently.

Sugar infusion alleviated root C limitation in pine but exacerbated it in maple

Without sugar infusion, fine root NSC concentrations in both species were significantly lower in C-limited trees than in non-C-limited trees (Fig. 4g,h). We found that fast sugar infusion in non-C-limited trees of both maple and pine led to a significant reduction in F_v/F_m, indicating some damage to photosystem II (Fig. 2m,n). This was paralleled by a decline in NSC concentrations in fine roots but not in leaves or twigs (Fig. 4g,h), highlighting that impaired photosynthesis primarily affected the fine roots' NSC levels. In maple, a larger proportion of infused sugars was transported to the leaves, leading to sugar accumulation (Figs 4a, S5). However, this was accompanied by a downregulation of photosynthesis (Fig. 2a) and the induction of senescence (Fig. S4). These factors led to an exacerbation of C limitation in the fine roots, as root NSC concentrations declined in response to C being actively reallocated to support new leaf development (Fig. 4g). Hence, adding exogenous sugars to the xylem did not relieve but intensified C limitation as a result of the impairment of photosynthesis in maple. By contrast, pine trees did not exhibit significant sugar accumulation in their needles (Fig. S5), maintained stable photosynthetic activity across treatments (Figs 2b, 4b), and showed potential for mitigating C limitation (increased NSC) in their fine roots (Fig. 4h). The ^{13}C analyses from respiration and cellulose further support the second hypothesis: Under fast sugar infusion, C-limited pines had significantly higher ^{13}C values in respiration and cellulose in fine roots than in non-C-limited pines (Figs 3, 7). This indicates that C-limited pines can allocate more exogenous C to structural growth, thereby improving their overall structural integrity and resource acquisition capabilities, and potentially mitigating C limitation. These findings support both hypotheses and highlight the high sensitivity of fine roots to C limitation, making it the initial organ affected by impaired photosynthesis. This aligns well with previous findings indicating that in large trees, roots are especially susceptible to C starvation when crown-level C assimilation is constrained or transport processes are disrupted, leading to prolonged and severe NSC deficits in roots (Landhäusser & Lieffers, 2002, 2012; Wiley *et al.*, 2017; W. Li *et al.*, 2018; Partelli-Feltrin *et al.*, 2023).

Implications for tree growth and recovery

Our study demonstrates that sugar infusion could alleviate root C limitation in young pine trees, provided photosynthesis remains unaffected. This crucial finding emphasizes the interplay between source activity (photosynthesis) and sink utilization (roots), which determines the efficacy of elevated exogenous sugar supply. Our results reveal that, in maples, the additional sugar supply can trigger feedback regulation on photosynthesis, exacerbating C limitation rather than alleviating it. We assume that the exogenous sugar supply interfered with the adjustment of source activity to sink demand, signaling excess sugar availability. This signal exerted immediate negative feedback on photosynthesis and led to a further step to leaf senescence. Thus, the short-term excess supply and transport of sugars to the leaf impaired photosynthetic capacity and therefore initiated or exacerbated existing root C limitation. By contrast, pine maintained photosynthesis and redirected exogenous sugars to fine roots, suggesting species-specific differences in sugar transport efficiency that influence tree survival strategies under C-limited conditions. Given that root C depletion is a major factor in tree mortality under C starvation (see Hunziker *et al.*, 2024), our study

highlights the importance of strategies that preserve photosynthesis to maintain root function.

Future studies ought to account for these species-dependent differences in sugar transport efficiency to refine C supplementation strategies including optimal sugar concentrations and amount. Moreover, whether these mechanisms apply across a broad range of tree species and whether different sugar forms (e.g. fructose and sucrose) with different metabolic pathways influence C allocation differently remains an open question. Additionally, the relevance of these findings to mature trees is uncertain, as older, taller trees generally possess larger NSC pools that may buffer against C limitation differently than saplings. Nevertheless, our study highlights photosynthetic impairment as a dominant driver of root C limitation and suggests that maintaining photosynthesis is a prerequisite for alleviating root C limitation through exogenous sugar addition.

Acknowledgements

Our work was supported by the Swiss Innovation Partnership Grants with East and Southeast Asia (project no. IPG 022023_3 to M-HL). Y-LZ was partly supported by the Chinese Scholarship Council (grant no. 202103270001). MML was funded by the Swiss National Science Foundation (SNSF, grant no. 213367). We thank Gabor Reiss, Peter Suter, and Claudio Cattaneo for their assistance in setting up the experimental platform and watering the trees in the glasshouse. We thank Dr Philipp Schuler, Dr Liangjun Zhu, Danyang Yuan, Yi Zhu, Dr Fang Wang, Dr Yuman Sun, Dr Zhaoyong Hu, and Dr Shaoting Ren (all from WSL) for their great support in sampling. We thank Manuela Oettli (WSL) for her laboratory assistance. We also thank Professor Janneke Hille Ris Lambers (ETH Zurich) for her valuable feedback and insightful suggestions, which significantly contributed to the improvement of this manuscript. We would like to thank the editor and the three anonymous reviewers for their thoughtful comments and constructive suggestions, which helped improve the manuscript.

Competing interests

None declared.

Author contributions

M-HL conceived the ideas and designed the methodology. M-HL and Y-LZ established the experiments. Y-LZ and M-HL carried out the experiment. Y-LZ collected, analyzed the data, and drafted the manuscript with constructive input from M-HL and AG. Y-LZ, M-HL, AG, MML, M Schaub, M Saurer, and AR interpreted the data and revised the manuscript. All the authors approved the final manuscript.

ORCID

Arthur Gessler https://orcid.org/0000-0002-1910-9589
Marco M. Lehmann https://orcid.org/0000-0003-2962-3351
Mai-He Li https://orcid.org/0000-0002-7029-2841
Andreas Rigling https://orcid.org/0000-0003-1944-4042
Matthias Saurer https://orcid.org/0000-0002-3954-3534
Marcus Schaub https://orcid.org/0000-0002-0158-8892
Yan-Li Zhang https://orcid.org/0000-0003-1738-4672

Data availability

All data used in this manuscript are available in the Supporting Information. Glasshouse data are presented in Figs S1 and S2, and all measured data are provided in Table S3.

References

Adler PB, Salguero-Gómez R, Compagnoni A, Hsu JS, Ray-Mukherjee J, Mbeau-Ache C, Franco M. 2014. Functional traits explain variation in plant life history strategies. *Proceedings of the National Academy of Sciences, USA* **111**: 740–745.

Allen CD, Macalady AK, Chenchouni H, Bachelet D, McDowell N, Vennetier M, Kitzberger T, Rigling A, Breshears DD, Hogg EH *et al.* 2010. A global overview of drought and heat-induced tree mortality reveals emerging climate change risks for forests. *Forest Ecology and Management* **259**: 660–684.

Anderegg WRL, Hicke JA, Fisher RA, Allen CD, Aukema J, Bentz B, Hood S, Lichstein JW, Macalady AK, McDowell N *et al.* 2015. Tree mortality from drought, insects, and their interactions in a changing climate. *New Phytologist* **208**: 674–683.

Aphalo PJ. 2021. *GGPMISC: Miscellaneous Extensions to 'ggplot2'*. R package v.0.3 3. [WWW document] URL https://cran.rstudio.com/web/packages/ggpmisc/.

Asao S, Way DA, Turnbull MH, Stitt M, McDowell NG, Reich PB, Bloomfield KJ, Zaragoza-Castells J, Creek D, O'Sullivan O *et al.* 2025. Leaf nonstructural carbohydrate residence time, not concentration, correlates with leaf functional traits following the leaf economic spectrum in woody plants. *New Phytologist* **246**: 1505–1519.

Barker Plotkin A, Blumstein M, Laflower D, Pasquarella VJ, Chandler JL, Elkinton JS, Thompson JR. 2021. Defoliated trees die below a critical threshold of stored carbon. *Functional Ecology* **35**: 2156–2167.

Bates D, Maechler M, Bolker B, Walker S. 2024. *LME4: linear mixed-effects models using 'Eigen' and S4* [WWW document] URL https://cran.r-project.org/web/packages/lme4/ [accessed 1 September 2024].

Bieleski RL, Ripperda J, Newman JP, Reid MS. 1992. Carbohydrate changes and leaf blackening in cut flower stems of *Protea eximia* **117**: 124–127.

Boyle MG, Boyer JS, Morgan PW. 1991. Stem infusion of liquid culture medium prevents reproductive failure of maize at low water potential. *Crop Science* **31**: 1246–1252.

Brodribb TJ, Powers J, Cochard H, Choat B. 2020. Hanging by a thread? Forests and drought. *Science* **368**: 261–266.

Didion-Gency M, Gessler A, Buchmann N, Gisler J, Schaub M, Grossiord C. 2022. Impact of warmer and drier conditions on tree photosynthetic properties and the role of species interactions. *New Phytologist* **236**: 547–560.

Duursma RA. 2015. Plantecophys - an R package for analysing and modelling leaf gas exchange data. *PLoS ONE* **10**: e0143346.

Eamus D, Prichard H. 1998. A cost-benefit analysis of leaves of four australian savanna species. *Tree Physiology* **18**: 537–545.

Esau K. 1977. *Anatomy of seed plants.* New York, NY, USA: Wiley.

Esau K. 2013. *Plants, Viruses, and Insects.* Cambridge, MA, USA: Harvard University Press.

Eyles A, Pinkard EA, Davies NW, Corkrey R, Churchill K, O'Grady AP, Sands P, Mohammed C. 2013. Whole-plant versus leaf-level regulation of photosynthetic responses after partial defoliation in *Eucalyptus globulus* saplings. *Journal of Experimental Botany* **64**: 1625–1636.

Eyles A, Pinkard EA, Mohammed C. 2009. Shifts in biomass and resource allocation patterns following defoliation in *Eucalyptus globulus* growing with varying water and nutrient supplies. *Tree Physiology* **29**: 753–764.

Farquhar GD, von Caemmerer S, Berry JA. 1980. A biochemical model of photosynthetic CO_2 assimilation in leaves of C_3 species. *Planta* **149**: 78–90.

Forrester DI, Tachauer IHH, Annighoefer P, Barbeito I, Pretzsch H, Ruiz-Peinado R, Stark H, Vacchiano G, Zlatanov T, Chakraborty T *et al.* 2017. Generalized biomass and leaf area allometric equations for European tree species incorporating stand structure, tree age and climate. *Forest Ecology and Management* **396**: 160–175.

Fotelli MN, Rennenberg H, Holst T, Mayer H, Geßler A. 2003. Carbon isotope composition of various tissues of beech (*Fagus sylvatica*) regeneration is indicative of recent environmental conditions within the forest understorey. *New Phytologist* **159**: 229–244.

Gao D, Joseph J, Werner RA, Brunner I, Zürcher A, Hug C, Wang A, Zhao C, Bai E, Meusburger K *et al.* 2021. Drought alters the carbon footprint of trees in soils—tracking the spatio-temporal fate of 13C-labelled assimilates in the soil of an old-growth pine forest. *Global Change Biology* **27**: 2491–2506.

Gaudinski JB, Dawson TE, Quideau S, Schuur EAG, Roden JS, Trumbore SE, Sandquist DR, Oh S-W, Wasylishen RE. 2005. Comparative analysis of cellulose preparation techniques for use with ^{13}C, ^{14}C, and ^{18}O Isotopic measurements. *Analytical Chemistry* **77**: 7212–7224.

Gessler A, Zweifel R. 2024. Beyond source and sink control – toward an integrated approach to understand the carbon balance in plants. *New Phytologist* **242**: 858–869.

Graf A, Schlereth A, Stitt M, Smith AM. 2010. Circadian control of carbohydrate availability for growth in Arabidopsis plants at night. *Proceedings of the National Academy of Sciences, USA* **107**: 9458–9463.

Groover A, Holbrook NM, Polle A, Sala A, Medlyn B, Brodersen C, Pittermann J, Gersony J, Sokołowska K, Bogar L *et al.* 2025. Tree drought physiology: critical research questions and strategies for mitigating climate change effects on forests. *New Phytologist* **245**: 1817–1832.

Hagedorn F, Joseph J, Peter M, Luster J, Pritsch K, Geppert U, Kerner R, Molinier V, Egli S, Schaub M *et al.* 2016. Recovery of trees from drought depends on belowground sink control. *Nature Plants* **2**: 1–5.

Hartmann H, Moura CF, Anderegg WRL, Ruehr NK, Salmon Y, Allen CD, Arndt SK, Breshears DD, Davi H, Galbraith D *et al.* 2018. Research frontiers for improving our understanding of drought-induced tree and forest mortality. *New Phytologist* **218**: 15–28.

Heizmann U, Kreuzwieser J, Schnitzler J-P, Brüggemann N, Rennenberg H. 2001. Assimilate transport in the xylem sap of pedunculate oak (*Quercus robur*) saplings. *Plant Biology* **3**: 132–138.

Hiyane R, Hiyane S, Tang AC, Boyer JS. 2010. Sucrose feeding reverses shade-induced kernel losses in maize. *Annals of Botany* **106**: 395–403.

Huang J, Hammerbacher A, Weinhold A, Reichelt M, Gleixner G, Behrendt T, van Dam NM, Sala A, Gershenzon J, Trumbore S *et al.* 2019. Eyes on the future – evidence for trade-offs between growth, storage and defense in Norway spruce. *New Phytologist* **222**: 144–158.

Hunziker S, Nazarova T, Kather M, Hartmann M, Brunner I, Schaub M, Rigling A, Hug C, Schönbeck L, Bose AK *et al.* 2024. The metabolic fingerprint of Scots pine—root and needle metabolites show different patterns in dying trees. *Tree Physiology* **44**: tpae036.

Iglesias DJ, Lliso I, Tadeo FR, Talon M. 2002. Regulation of photosynthesis through source: sink imbalance in citrus is mediated by carbohydrate content in leaves. *Physiologia Plantarum* **116**: 563–572.

Iglesias DJ, Tadeo FR, Primo-Millo E, Talon M. 2003. Fruit set dependence on carbohydrate availability in citrus trees. *Tree Physiology* **23**: 199–204.

International Tree Mortality Network. 2025. Towards a global understanding of tree mortality. *New Phytologist* **245**: 2377–2392.

Joseph J, Gao D, Backes B, Bloch C, Brunner I, Gleixner G, Haeni M, Hartmann H, Hoch G, Hug C *et al.* 2020. Rhizosphere activity in an old-growth forest reacts rapidly to changes in soil moisture and shapes whole-tree carbon allocation. *Proceedings of the National Academy of Sciences, USA* **117**: 24885–24892.

Keeling CD. 1961. The concentration and isotopic abundances of carbon dioxide in rural and marine air. *Geochimica et Cosmochimica Acta* **24**: 277–298.

Körner C. 2015. Paradigm shift in plant growth control. *Current Opinion in Plant Biology* **25**: 107–114.

Krapp A, Quick WP, Stitt M. 1991. Ribulose-1,5-bisphosphate carboxylase-oxygenase, other Calvin-cycle enzymes, and chlorophyll decrease when glucose is supplied to mature spinach leaves via the transpiration stream. *Planta* **186**: 58–69.

Kumar R, Bishop E, Bridges WC, Tharayil N, Sekhon RS. 2019. Sugar partitioning and source–sink interaction are key determinants of leaf senescence in maize. *Plant, Cell & Environment* **42**: 2597–2611.

Landhäusser SM, Chow PS, Dickman LT, Furze ME, Kuhlman I, Schmid S, Wiesenbauer J, Wild B, Gleixner G, Hartmann H *et al.* 2018. Standardized protocols and procedures can precisely and accurately quantify non-structural carbohydrates. *Tree Physiology* **38**: 1764–1778.

Landhäusser SM, Lieffers VJ. 2002. Leaf area renewal, root retention and carbohydrate reserves in a clonal tree species following above-ground disturbance. *Journal of Ecology* **90**: 658–665.

Landhäusser SM, Lieffers VJ. 2012. Defoliation increases risk of carbon starvation in root systems of mature aspen. *Trees* **26**: 653–661.

Lemoine R, La Camera S, Atanassova R, Dédaldéchamp F, Allario T, Pourtau N, Bonnemain J-L, Laloi M, Coutos-Thévenot P, Maurousset L *et al.* 2013. Source-to-sink transport of sugar and regulation by environmental factors. *Frontiers in Plant Science* **4**: 272.

Li M-H, Jiang Y, Wang A, Li X, Zhu W, Yan C-F, Du Z, Shi Z, Lei J, Schönbeck L *et al.* 2018. Active summer carbon storage for winter persistence in trees at the cold alpine treeline. *Tree Physiology* **38**: 1345–1355.

Li W, Hartmann H, Adams HD, Zhang H, Jin C, Zhao C, Guan D, Wang A, Yuan F, Wu J. 2018. The sweet side of global change–dynamic responses of non-structural carbohydrates to drought, elevated CO_2 and nitrogen fertilization in tree species. *Tree Physiology* **38**: 1706–1723.

Lobo AKM, de Oliveira Martins M, Lima Neto MC, Machado EC, Ribeiro RV, Silveira JAG. 2015. Exogenous sucrose supply changes sugar metabolism and reduces photosynthesis of sugarcane through the down-regulation of Rubisco abundance and activity. *Journal of Plant Physiology* **179**: 113–121.

Mai MH, Gao C, Bork PAR, Holbrook NM, Schulz A, Bohr T. 2024. Relieving the transfusion tissue traffic jam: a network model of radial transport in conifer needles. *New Phytologist* **244**: 2183–2196.

Martínez-Trinidad T, Watson WT, Arnold MA, Lombardini L, Appel DN. 2009. Carbohydrate injections as a potential option to improve growth and vitality of live oaks. *Arboriculture & Urban Forestry* **35**: 142–147.

McCormick AJ, Cramer MD, Watt DA. 2008. Regulation of photosynthesis by sugars in sugarcane leaves. *Journal of Plant Physiology* **165**: 1817–1829.

McDowell N, Pockman WT, Allen CD, Breshears DD, Cobb N, Kolb T, Plaut J, Sperry J, West A, Williams DG *et al.* 2008. Mechanisms of plant survival and mortality during drought: why do some plants survive while others succumb to drought? *New Phytologist* **178**: 719–739.

McDowell NG, Sapes G, Pivovaroff A, Adams HD, Allen CD, Anderegg WRL, Arend M, Breshears DD, Brodribb T, Choat B *et al.* 2022. Mechanisms of woody-plant mortality under rising drought, CO_2 and vapour pressure deficit. *Nature Reviews Earth and Environment* **3**: 294–308.

Miller A, Tsai CH, Hemphill D, Endres M, Rodermel S, Spalding M. 1997. Elevated CO_2 effects during leaf ontogeny (a new perspective on acclimation). *Plant Physiology* **115**: 1195–1200.

Moore BD, Cheng S-H, Sims D, Seemann JR. 1999. The biochemical and molecular basis for photosynthetic acclimation to elevated atmospheric CO_2. *Plant, Cell & Environment* **22**: 567–582.

Neales TF, Incoll LD. 1968. The control of leaf photosynthesis rate by the level of assimilate concentration in the leaf: a review of the hypothesis. *The Botanical Review* **34**: 107–125.

Nebauer SG, Renau-Morata B, Guardiola JL, Molina R-V. 2011. Photosynthesis down-regulation precedes carbohydrate accumulation under sink limitation in Citrus. *Tree Physiology* **31**: 169–177.

Ouyang S-N, Gessler A, Saurer M, Hagedorn F, Gao D-C, Wang X-Y, Schaub M, Li M-H, Shen W-J, Schönbeck L. 2021. Root carbon and nutrient homeostasis determines downy oak sapling survival and recovery from drought. *Tree Physiology* **41**: 1400–1412.

Ozawa Y, Tanaka A, Suzuki T, Sugiura D. 2023. Sink–source imbalance triggers delayed photosynthetic induction: transcriptomic and physiological evidence. *Physiologia Plantarum* **175**: e14000.

Palacio S, Camarero JJ, Maestro M, Alla AQ, Lahoz E, Montserrat-Martí G. 2018. Are storage and tree growth related? Seasonal nutrient and carbohydrate dynamics in evergreen and deciduous mediterranean oaks. *Trees* **32**: 777–790.

Parry C, Blonquist JM Jr, Bugbee B. 2014. In situ measurement of leaf chlorophyll concentration: analysis of the optical/absolute relationship. *Plant, Cell & Environment* **37**: 2508–2520.

Partelli-Feltrin R, Smith AMS, Adams HD, Thompson RA, Kolden CA, Yedinak KM, Johnson DM. 2023. Death from hunger or thirst? Phloem death, rather than xylem hydraulic failure, as a driver of fire-induced conifer mortality. *New Phytologist* **237**: 1154–1163.

Paul MJ, Foyer CH. 2001. Sink regulation of photosynthesis. *Journal of Experimental Botany* **52**: 1383–1400.

Pedersen TL. 2022. *PATCHWORK: the composer of plots.* [WWW document] URL https://github.com/thomasp85/patchwork [accessed 22 August 2023].

Pinkard EA, Eyles A, O'grady AP. 2011. Are gas exchange responses to resource limitation and defoliation linked to source:sink relationships? *Plant, Cell & Environment* **34**: 1652–1665.

Plavcová L, Jansen S. 2015. The role of xylem parenchyma in the storage and utilization of nonstructural carbohydrates. In: Hacke U, ed. *Functional and ecological xylem anatomy.* Cham, Switzerland: Springer International Publishing, 209–234.

R Core Team. 2024. *R: a language and environment for statistical computing.* Vienna, Austria: R Foundation for Statistical Computing. [WWW document] URL https://www.R-project.org/.

Rademacher T, Fonti P, LeMoine JM, Fonti MV, Bowles F, Chen Y, Eckes-Shephard AH, Friend AD, Richardson AD. 2022. Insights into source/sink controls on wood formation and photosynthesis from a stem chilling experiment in mature red maple. *New Phytologist* **236**: 1296–1309.

Rani A, Zhao Y, Yan Q, Wang Y, Ma R, Zhu Z, Wang B, Li T, Zhou X, Hocart CH *et al.* 2023. On the chemical purity and oxygen isotopic composition of α-cellulose extractable from higher plants and the implications for climate, metabolic, and physiological studies. *Analytical Chemistry* **95**: 4871–4879.

Raven JA. 1983. Phytophages of xylem and phloem: a comparison of animal and plant sap-feeders. In: MacFadyen A, Ford ED, eds. *Advances in ecological research.* New York, NY, USA: Academic Press, 135–234.

Reich PB. 2014. The world-wide 'fast–slow' plant economics spectrum: a traits manifesto. *Journal of Ecology* **102**: 275–301.

Ruehr NK, Offermann CA, Gessler A, Winkler JB, Ferrio JP, Buchmann N, Barnard RL. 2009. Drought effects on allocation of recent carbon: from beech leaves to soil CO_2 efflux. *New Phytologist* **184**: 950–961.

Sade N, del Mar Rubio-Wilhelmi M, Umnajkitikorn K, Blumwald E. 2018. Stress-induced senescence and plant tolerance to abiotic stress. *Journal of Experimental Botany* **69**: 845–853.

Salguero-Gómez R. 2017. Applications of the fast–slow continuum and reproductive strategy framework of plant life histories. *New Phytologist* **213**: 1618–1624.

Schönbeck L, Gessler A, Hoch G, McDowell NG, Rigling A, Schaub M, Li M-H. 2018. Homeostatic levels of nonstructural carbohydrates after 13 yr of drought and irrigation in *Pinus sylvestris*. *New Phytologist* **219**: 1314–1324.

Schönbeck L, Gessler A, Schaub M, Rigling A, Hoch G, Kahmen A, Li M-H. 2020. Soil nutrients and lowered source:sink ratio mitigate effects of mild but not of extreme drought in trees. *Environmental and Experimental Botany* **169**: 103905.

Senf C, Pflugmacher D, Zhiqiang Y, Sebald J, Knorn J, Neumann M, Hostert P, Seidl R. 2018. Canopy mortality has doubled in Europe's temperate forests over the last three decades. *Nature Communications* **9**: 4978.

Senf C, Sebald J, Seidl R. 2021. Increasing canopy mortality affects the future demographic structure of Europe's forests. *One Earth* **4**: 749–755.

Sharkey TD, Bernacchi CJ, Farquhar GD, Singsaas EL. 2007. Fitting photosynthetic carbon dioxide response curves for C3 leaves. *Plant, Cell & Environment* **30**: 1035–1040.

Smith AM, Stitt M. 2007. Coordination of carbon supply and plant growth. *Plant, Cell and Environment* **30**: 1126–1149.

Tian M, Salmon Y, Lintunen A, Oren R, Hölttä T. 2024. Seasonal dynamics and punctuated carbon sink reduction suggest photosynthetic capacity of boreal silver birch is reduced by the accumulation of hexose. *New Phytologist* **243**: 894–908.

Van Bel AJE. 1990. Xylem–phloem exchange via the rays: the undervalued route of transport. *Journal of Experimental Botany* **41**: 631–644.

Wang X, Yu F-H, Jiang Y, Li M-H. 2021. Carbon and nutrient physiology in shrubs at the upper limits: a multispecies study. *Journal of Plant Ecology* **14**: 301–309.

Wang Z, Zhou Z, Wang C. 2021. Defoliation-induced tree growth declines are jointly limited by carbon source and sink activities. *Science of the Total Environment* **762**: 143077.

Weber R, Gessler A, Hoch G. 2019. High carbon storage in carbon-limited trees. *New Phytologist* **222**: 171–182.

Wickham H. 2016. *GGPLOT2: elegant graphics for data analysis.* New York, NY, USA: Springer-Verlag.

Wiley E, Helliker B. 2012. A re-evaluation of carbon storage in trees lends greater support for carbon limitation to growth. *New Phytologist* **195**: 285–289.

Wiley E, Hoch G, Landhäusser SM. 2017. Dying piece by piece: carbohydrate dynamics in aspen (*Populus tremuloides*) seedlings under severe carbon stress. *Journal of Experimental Botany* **68**: 5221–5232.

Wu X, Lin J, Lin Q, Wang J, Schreiber L. 2005. Casparian strips in needles are more solute permeable than endodermal transport barriers in roots of *Pinus bungeana*. *Plant and Cell Physiology* **46**: 1799–1808.

Yang Y, Ouyang S, Gessler A, Wang X, Na R, He HS, Wu Z, Li M-H. 2022. Root carbon resources determine survival and growth of young trees under long drought in combination with fertilization. *Frontiers in Plant Science* **13**: 929855.

Zani D, Crowther TW, Mo L, Renner SS, Zohner CM. 2020. Increased growing-season productivity drives earlier autumn leaf senescence in temperate trees. *Science* **370**: 1066–1071.

Zhang Y-L, Moser B, Li M-H, Wohlgemuth T, Lei J-P, Bachofen C. 2020. Contrasting leaf trait responses of conifer and broadleaved seedlings to altered resource availability are linked to resource strategies. *Plants* **9**: 621.

Zhang Y-L, Yang Y, Saurer M, Schaub M, Gessler A, Lehmann MM, Rigling A, Walser M, Stierli B, Hajjar N *et al.* 2023. Sugar infusion into trees: a novel method to study tree carbon relations and its regulations. *Frontiers in Plant Science* **14**: 1142595.

Supporting Information

Additional Supporting Information may be found online in the Supporting Information section at the end of the article.

Fig. S1 Light condition during experiments in the glasshouse.

Fig. S2 Room temperature and humidity conditions during experiments in the glasshouse.

Fig. S3 Leaf nonstructural C residence time in response to sugar infusion, defoliation, and species.

Fig. S4 Visual effects of sugar infusion treatments on the phenology of sycamore maple and Scots pine.

Fig. S5 Estimation of the amount of infused sugar transported to leaves in a day in sycamore maple and Scots pine.

Fig. S6 Estimation of the proportion of infused sugar in nonleaf organs (%) in a day in sycamore maple and Scots pine.

Table S1 Summary of the ANOVA tests of the linear mixed-effects models with the effects of species, defoliation, and water infusion treatments on the measured traits.

Table S2 Summary of the ANOVA tests of the linear mixed-effects models with the effects of species, defoliation, and sugar infusion treatments on the measured traits.

Table S3 Data on measured traits comparing C-limited and non-C-limited trees.

Table S4 Summary of the ANOVA tests of the linear mixed-effects models with the effects of species, defoliation, sugar infusion, and tissue on the amount of enriched ^{13}C in cellulose.

Please note: Wiley is not responsible for the content or functionality of any Supporting Information supplied by the authors. Any queries (other than missing material) should be directed to the *New Phytologist* Central Office.